



**UNIVERSITY OF LEEDS**

This is a repository copy of *Meandering rivers in modern desert basins: Implications for channel planform controls and prevegetation rivers*.

White Rose Research Online URL for this paper:  
<http://eprints.whiterose.ac.uk/144645/>

Version: Accepted Version

---

**Article:**

Santos, MGM, Hartley, AJ, Mountney, NP [orcid.org/0000-0002-8356-9889](https://orcid.org/0000-0002-8356-9889) et al. (4 more authors) (2019) Meandering rivers in modern desert basins: Implications for channel planform controls and prevegetation rivers. *Sedimentary Geology*, 385. pp. 1-14. ISSN 0037-0738

<https://doi.org/10.1016/j.sedgeo.2019.03.011>

---

© 2019 Elsevier B.V. All rights reserved. Licensed under the Creative Commons Attribution-Non Commercial No Derivatives 4.0 International License (<https://creativecommons.org/licenses/by-nc-nd/4.0/>).

**Reuse**

This article is distributed under the terms of the Creative Commons Attribution-NonCommercial-NoDerivs (CC BY-NC-ND) licence. This licence only allows you to download this work and share it with others as long as you credit the authors, but you can't change the article in any way or use it commercially. More information and the full terms of the licence here: <https://creativecommons.org/licenses/>

**Takedown**

If you consider content in White Rose Research Online to be in breach of UK law, please notify us by emailing [eprints@whiterose.ac.uk](mailto:eprints@whiterose.ac.uk) including the URL of the record and the reason for the withdrawal request.



[eprints@whiterose.ac.uk](mailto:eprints@whiterose.ac.uk)  
<https://eprints.whiterose.ac.uk/>

# 1 Meandering rivers in modern desert basins: implications for 2 channel planform controls and prevegetation rivers

3 Mauricio G.M. Santos<sup>1\*</sup>, Adrian J. Hartley<sup>2</sup>, Nigel P. Mountney<sup>3</sup>, Jeff Peakall<sup>3</sup>, Amanda Owen<sup>4</sup>,  
4 Eder R. Merino<sup>5</sup>, Mario L. Assine<sup>6</sup>

5 <sup>1</sup>CECS, Universidade Federal do ABC (UFABC), Av. dos Estados 5001, Santo André, Brazil, CEP 09210-580, Brazil.

6 <sup>2</sup>Department of Geology and Petroleum Geology, University of Aberdeen, Aberdeen AB24 3UE, UK.

7 <sup>3</sup>School of Earth and Environment, University of Leeds, Leeds LS2 9JT, UK.

8 <sup>4</sup>School of Geographical and Earth Sciences, University of Glasgow, University Avenue, Glasgow, 8NN, UK.

9 <sup>5</sup>Institute of Energy and Environment, USP, Av. Professor Luciano Gualberto 1289, Cidade Universitária, CEP 05508-010, Brazil.

10 <sup>6</sup>Instituto de Geociências e Ciências Exatas, UNESP, Avenida 24A 1515, Rio Claro, CEP 13.506-900, Brazil.

11

12 \*Corresponding author. *E-mail address:* mauriciogmsantos@gmail.com

13

## 14 **A B S T R A C T**

15 The influence of biotic processes in controlling the development of meandering channels in  
16 fluvial systems is controversial. The majority of the depositional history of the Earth's continents  
17 was devoid of significant biogeomorphic interactions, particularly those between vegetation and  
18 sedimentation processes. The prevailing perspective has been that prevegetation meandering  
19 channels rarely developed and that rivers with braided planforms dominated. However, recently  
20 acquired data demonstrate that meandering channel planforms are more widely preserved in  
21 prevegetation fluvial successions than previously thought. Understanding the role of prevailing  
22 fluvial dynamics in non- and poorly vegetated environments must rely on actualistic models  
23 derived from presently active rivers developed in sedimentary basins subject to desert-climate  
24 settings, the sparsest vegetated regions experiencing active sedimentation on Earth. These  
25 systems have fluvial depositional settings that most closely resemble those present in  
26 prevegetation (and extra-terrestrial) environments. Here, we present an analysis based on satellite  
27 imagery which reveals that rivers with meandering channel planforms are common in modern

28 sedimentary basins in desert settings. Morphometric analysis of meandering fluvial channel  
29 behaviour, where vegetation is absent or highly restricted, shows that modern sparsely and non-  
30 vegetated meandering rivers occur across a range of slope gradients and basin settings, and  
31 possess a broad range of channel and meander-belt dimensions. The importance of meandering  
32 rivers in modern desert settings suggests that their abundance is likely underestimated in the  
33 prevegetation rock record, and models for recognition of their deposits need to be improved.

34 *Keywords:* Meandering rivers; arid sedimentary basins; prevegetation fluvial deposits; remote  
35 sensing; modern analogues; dryland.

## 36 **1. Introduction**

37         Assessment of the biotic and abiotic controls on channel-planform development in  
38 alluvial rivers is a fundamental objective in fluvial sedimentology (Wolman and Brush, 1961;  
39 Leopold et al., 1965; Schumm, 1968; Peakall et al., 2007; Jansen and Nanson, 2010), and  
40 particularly in the geology of preserved fluvial deposits (Long, 1978, 2006, 2011; Sønderholm  
41 and Tirsgaard, 1998; Eriksson et al., 2006; Santos et al., 2014; Ielpi et al., 2017a; McMahon and  
42 Davies, 2017). A related research question is to what extent did the presence of vegetation in  
43 continental environments induce the development of single-channel, meandering planforms and  
44 the preservation of laterally-accreting strata (Davies and Gibling, 2010; Davies et al., 2017;  
45 Santos et al., 2017a,b)? Experimental studies of fluvial systems using laboratory-based flume  
46 apparatus have provided evidence which indicates that, although the presence of vegetation is  
47 believed to encourage fluvial systems to develop meandering planforms (Braudrick et al., 2009;  
48 Tal and Paola, 2010), vegetation is not a requirement for the growth and preservation of point-  
49 bar deposits associated with meandering river behaviour (Peakall et al., 2007; Van de Lageweg et  
50 al., 2014). Recent studies have highlighted the abundance of relict and potentially active flow-  
51 related features which were also apparently related to meander development in non-vegetated  
52 landscapes on other planetary bodies, including Mars and Titan (Schon et al., 2012; Burr et al.,

53 2013; Matsubara et al., 2015). These observations contrast with the hypothesis that non-  
54 vegetated meandering rivers rarely developed in the pre-Silurian on Earth (Vogt, 1941; Cotter,  
55 1978; Long, 1978; Davies and Gibling, 2010), and that most prevegetation river channels were  
56 typified by braided planform morphologies characterized by shallow and wide channels (Cotter,  
57 1978; Long, 1978, 2011). Ideas that prevegetation systems were subject to lower river-bank  
58 stability and flashy runoff characterized by markedly peaked flood hydrographs (Schumm, 1968),  
59 lead to commonly observed biases on the interpretations of prevegetation river deposits in the  
60 literature (Ethridge, 2011).

61         Few environments in modern aggradational settings are entirely devoid of vegetation.  
62 Although the intrinsic association between life and water means that vegetation will inevitably  
63 develop where rivers are present, the density of vegetation cover can vary according to climatic  
64 conditions, with climatic deserts being the least vegetated continental environments in which  
65 rivers develop. The understanding of meandering rivers developed in subsiding desert  
66 sedimentary basins thus provides the best opportunity to assess not only how these rivers can  
67 develop with little to no vegetation, but also the plausibility of their occurrence on the  
68 prevegetated Earth.

69         Although braided channels are commonly considered to be the prevailing channel  
70 planform in drylands (Tooth, 2000), recent work has highlighted the geomorphology of  
71 ephemeral meandering rivers (Billi et al., 2018) and also meandering rivers developed in poorly  
72 vegetated environments such as those that host aeolian dunes fields, proglacial rivers (e.g. sandur  
73 plains in Iceland), and salt flats (Almasrahy and Mountney, 2015; Li and Bristow, 2015; Li et al.,  
74 2015; Ielpi, 2017b,c, 2019). However, there has hitherto been no systematic study of the  
75 worldwide distribution, prevalence, and characteristics of meandering rivers in modern arid  
76 sedimentary basins.

77 Here we identify and characterize the morphology of selected meandering rivers in a  
78 variety of desert basins with little to no vegetation. We seek to determine the ability of rivers to  
79 meander without vegetation present, and to assess what this means for prevegetation river  
80 behaviour. Specific research objectives are to understand the following: (i) the characteristics of  
81 major meandering fluvial systems developed with little to no vegetation; (ii) how restricted  
82 vegetation is in modern meandering river systems which are present in deserts on Earth; (iii) the  
83 controls that maintain meandering rivers with restricted vegetation; and (iv) if any of these  
84 meandering rivers are potential analogues for rivers in prevegetation systems.

## 85 **2. Methods**

### 86 *2.1. Global identification of meandering rivers on modern desert basins*

87 Modern depositional areas with the most limited vegetation on Earth have been analysed  
88 using Google Earth to identify representative meandering channel planforms; we selected rivers  
89 of basin-scale dimensions and with little or no anthropogenic influence. Sixteen meandering river  
90 systems developed in 12 modern sedimentary basins from different tectonic settings (Nyberg and  
91 Howell, 2015) developed under hot and cold desert climates (Kottke et al., 2006) from 5  
92 continents have been studied (Fig. 1). Analysed river lengths varied between 10 and 400 km;  
93 laterally-amalgamated meander belts were between 1 and 60 km wide, and channels varied from  
94 10 to 900 m in width (Table 1).

95 Selected rivers were analysed using GIS software to extract the following morphometric  
96 parameters: thalweg length, meander-belt length and width, channel sinuosity and planform  
97 pattern, main channel width, and stream gradient (Table 1; Supplementary Fig. S1). River  
98 gradient was calculated using Shuttle Radar Topography Mission (SRTM;  
99 <http://www.jpl.nasa.gov/srtm>) elevation data, version 4.1 (Jarvis et al., 2008) with 3 arc-seconds  
100 of spatial resolution (~90 m), with linear vertical relative height error less than 10 m for 90% of

101 the data (Rodríguez et al., 2005); the reported error in these data is chiefly concentrated in  
102 mountainous regions (see Hirt, 2018).

103 Meander belts were identified as channel belts (thalweg and internal bars) and bends;  
104 meander-belt and channel width were measured at regular intervals (every 20 km for > 200 km-  
105 long rivers, and every 10 km for smaller rivers). River sinuosity was defined as the ratio of  
106 channel length (along channel centre path) to straight-line down-valley distance, in which rivers  
107 with sinuosity <1.1 were classified as straight, those with a sinuosity of 1.1-1.5 were classified as  
108 low sinuosity, and those with sinuosity  $\geq 1.5$  were classified as meandering (Leopold et al., 1965).

## 109 2.2. Vegetation cover classification

110 The presence of vegetation in the selected alluvial plains was identified through analysis  
111 of satellite images with high and medium spatial resolution. Vegetation classification was  
112 performed using different types of satellite imagery depending on the scale of the selected river  
113 reach. Large-scale reaches were analysed using Landsat 8 OLI (false colour composite bands  
114 RGB 753, 654 and 543) with 30 m spatial resolution. For smaller reaches, GeoEye (0.46 m  
115 spatial resolution) georeferenced snapshots acquired using the World Imagery plug-in were used  
116 (ESRI, 2013). Calculation of cover percentage of vegetation types (palustrine or grasses) was  
117 performed through supervised classification of medium- and high-resolution images using the  
118 "Maximum likelihood classification" method on ArcGIS 10.2.2 (ESRI, 2013). The images were  
119 usually segmented in three classes (vegetation, water and soil), but some areas required the use of  
120 additional subclasses (i.e., vegetation 1 and 2, water 1 and 2, soil 1 and 2) to achieve a better  
121 image classification.

122 Vegetation cover percentage was computed for each active meander belt, where there is a  
123 clear segmentation between the latter and surrounding areas (Fig. 2); otherwise, vegetation cover  
124 across the entire alluvial plain was computed. Additionally, we have also separately calculated the  
125 vegetation cover on areas with no current fluvial sedimentation and also the total area of the

126 analysed examples, which includes both the surrounding areas and the active meander belt (Table  
127 1). These surrounding areas can be characterized by other ongoing sedimentation processes (e.g.,  
128 non-confined runoff, aeolian re-working) or by exposed, older meander-belt and lacustrine  
129 deposits (e.g. flat valley-bottom topography).

130 Variations between dry and rainy seasons and morphological details were acquired from  
131 recently released Planet images (Planet Team, 2017), with 3 m spatial resolution. Dry and rainy  
132 periods were identified using CHIRPS (Climate Hazards Group InfraRed Precipitation with  
133 Station Data) (Funk et al., 2015) on the Google Earth Engine (GEE) environment. The Google  
134 Earth Engine was also used to create time-lapse imagery (see supplemental materials) of each  
135 area using the Landsat collection from 1984 to present.

### 136 **3. Results**

#### 137 3.1. Meandering rivers in modern desert basins - overview

138 Sinuosity of the studied rivers ranges from 1.5 to 2.4, slope gradients from  $9 \times 10^{-6}$  to  $2 \times 10^{-}$   
139 <sup>3</sup>, and vegetation cover from 0 to 38% on the analysed meander belts (Table 1). Eleven of the  
140 studied systems developed laterally to, and were confined by, aeolian dunes. Scrolls, identified as  
141 crescent-shaped ridges and swales preserved along the inner channel banks, are recorded on a  
142 variety of scales (Fig. 3A, 3B), as are channel cut-offs (Fig. 3C) and oxbow lakes (Fig. 3A, 3D).  
143 Crevasses and crevasse splays are rare features in the studied examples, and develop in only two  
144 of the analysed systems: the Inner Niger Delta (Fig. 3B) and the Warburton River (Fig. 3C).  
145 Preserved scroll features are abundant in some examples (e.g. Senegal River) but are sparse in the  
146 other examples. In the Senegal River (Fig. 2A), which is fed by an equatorial climate in its source  
147 areas, vegetation follows scrolls and more recent deposits, particularly on river banks and on the  
148 inner parts of point bars. Small channels on the channel belt of the Senegal River shift laterally to  
149 erode the edge of vegetation-free aeolian dune fields and yet are able to develop meandering  
150 planforms (upper part of Fig. 3D).

151           Some of the studied examples are characterized by ephemeral flow (e.g., Amargosa  
152 River), others by perennial flow (e.g. Helmand River), and others are characterized by catchment  
153 areas with climatic regimes that differ from that of the depositional site (e.g., Senegal River). Yet,  
154 in all these different flow regimes, meandering rivers are able to develop with limited vegetation  
155 presence.

### 156 3.2 Geomorphology of meandering rivers in deserts

157           An abandoned contributory river to the Tarim River preserves multiple scrolls and  
158 abandoned-channel features (Fig. 4A). The example from Chad (Fig. 4B) is characterized by an  
159 abandoned or ephemeral system which flowed onto the exposed area of the extinct Lake Chad  
160 (Drake et al., 2011); it shows how fine-grained sediments can provide sufficient cohesion to  
161 stabilize river banks, even with very limited vegetation. Similarly, the Helmand River  
162 (Afghanistan) (Fig. 4C) meanders across a valley bottom composed of Neogene deposits of  
163 fluvial sand and silt, lacustrine silt and clay, and aeolian sand. These rivers develop in endorheic,  
164 intracratonic and foreland basin settings.

165           In rivers developed in siliciclastic environments, surrounding areas can either be largely  
166 devoid of aeolian dunes such as in the Bermejo River (Fig. 4D), or may be partly occupied by  
167 dune fields, such as in parts of the Senegal River. Areas with no currently active fluvial  
168 sedimentation are commonly dominated by aeolian processes, with the presence of aeolian dunes  
169 in 10 examples; vegetation presence in this setting ranges from 0 to 7%. Examples from Bolivia  
170 and Death Valley (USA) are exceptions whereby aeolian dunes did not develop on areas  
171 surrounding the active meander belt, with these rivers being developed in evaporitic settings: salt  
172 may have provided additional cohesion to induce meandering and scroll development (e.g.,  
173 Matsubara et al., 2015).

174           The Inner Niger Delta is characterized by a single-channel trunk system (Fig. 5A) with  
175 multiple tributaries with varying sinuosities (Fig. 5B) and varying dimensions (Fig. 5 C, D);

176 abundant scroll bars and sparse crevasses are recorded. Such tributaries commonly flow into  
177 rectilinear interdune settings and yet develop highly sinuous single channels (Fig. 5E).

178 The Warburton River in Lake Eyre displays crevasse development (Fig. 3C, 6A, 6B)  
179 where flow overflows levées and develops floodplain lakes such as the Perra Mudla Yeppa Lake.  
180 The river is entrenched into, and surrounded by, areas with aeolian-dominated landforms (Fig.  
181 6C), and also areas with developing channel-scrolls (Fig. 6D), abandoned channels and channel  
182 cut-offs (Fig. 6E).

### 183 3.3 Meandering as a function of tectono-climatic conditions and vegetation cover

184 The studied rivers develop in a variety of tectonic settings: foreland (Fig. 4A),  
185 intracratonic (Fig. 4B), pull-apart, and rift basins. They also develop in both cold (Fig. 4C) and  
186 hot (Fig. 4D) deserts. No significant differences between rivers developed in hot and cold desert  
187 climates is observable in terms of planform development and sinuosity (Table 1). The studied  
188 examples are stable at the scale of decades, as observed through time-lapse analysis using the  
189 Google Earth Engine (e.g., the Helmand River in Afghanistan: see multi-temporal links in  
190 Supplementary files). The meandering rivers we describe occupy large areas in the basin, tend to  
191 occur downstream of the point where the river enters a subsiding basin, and in an axial position  
192 in the basin, where surrounding sediment is largely distal alluvium or aeolian. In contrast to this,  
193 our observations show that, in most modern desert basins, braided systems form around the  
194 basin margins and have short-headed drainage catchments that supply fan-shaped bodies of  
195 sediment that are largely restricted in most cases to the basin flanks.

196 The presence of vegetation surface cover (Table 1) in the studied rivers varies from 0 to  
197 39% in meander belts, from 0 to 7% in the laterally adjacent areas, and from 0 to 18% in the  
198 total studied area. Although potential time-lag effects may be present, there is no correlation in  
199 these rivers between channel sinuosity and vegetation cover (Fig. 7) in: (i) meander belt; (ii)

200 surrounding areas of the meander belt; and (iii) total studied area (i + ii). Pearson's R ranges  
201 from -0.006 to 0.289.

202 The Inner Niger Delta (Mali) illustrates this lack of correlation: of the rivers considered  
203 in this study it has the second highest vegetation density on its meander belt (32%), the highest  
204 vegetation value for the total alluvial plain area (18%) and the adjacent area (7%), but it has the  
205 lowest sinuosity values of just 1.5. In contrast, the Zhanadarya River (Fig. 3A) has the second  
206 highest sinuosity value (1.8) and yet has extremely sparse vegetation cover on its meander belt  
207 (2%). The only system with a greater sinuosity is the Yobe river (Nigeria and Chad) with a  
208 sinuosity of 2.4; this has a far more densely vegetated meander belt (39%).

209 Importantly, many systems with no vegetation cover can develop meandering channels,  
210 and with different agents and mechanisms acting to provide cohesion other than vegetation. The  
211 studied example from the Bolivian Altiplano (Fig. 8A), is devoid of appreciable vegetation cover  
212 and yet develops features typical of meandering rivers, including oxbow lakes and preserved  
213 scrolls. The Amargosa River in the Death Valley (Fig. 8B) similarly is devoid of appreciable  
214 vegetation cover and develops highly sinuous single channels. These two systems are both  
215 characterized by evaporitic floodplain sediments, which give rise to cohesive properties that  
216 encourage channel-bank stabilization (e.g. Li et al., 2015; Ielpi, 2019). In addition, an ephemeral  
217 contributory of the Tarim River (Fig. 8C) is characterized by sandy and silty material (Li et al.,  
218 2017) and yet has been able to develop a similar channel sinuosity (1.7) to the aforementioned  
219 rivers developed in evaporitic settings. Additionally, no significant relationship between sinuosity  
220 and gradient (Fig. 7D) was identified (Pearson's R = -0.2201).

## 221 **4. Discussion**

### 222 4.1. Distribution of meandering rivers in modern sedimentary basins

223 Meandering channel systems are widespread features in modern desert basins, despite the  
224 absence or restriction of bank stabilization and runoff control by vegetation. Our data show no  
225 correlation between sinuosity and vegetation cover (Fig. 7). Furthermore, many such rivers flow  
226 through areas with varying vegetation-cover density, including vegetated areas and areas with no  
227 vegetation, with no observable changes on the overall appearance of channel organization (e.g.,  
228 Senegal River). The studied meandering rivers show that the presence of vegetation is not  
229 mandatory for development of a meandering planform, in contrast to traditional models for pre-  
230 vegetation river deposits which assumed that meandering river channels were rarely able to  
231 develop prior to the Silurian (Schumm, 1968; Davies and Gibling, 2010; Long, 2011; McMahon  
232 and Davies, 2017, 2018; Went and McMahon, 2018), and which favour the ubiquitous presence  
233 of shallow and wide braided channels, i.e., the sheet-braided fluvial style (Cotter, 1978).  
234 However, our results are in accordance with more recent models for prevegetation fluvial  
235 deposits which propose that not only were meandering channels able to develop before land-  
236 plant colonization (Santos and Owen, 2016) but they were also able to develop more variable  
237 river dynamics (e.g. Santos et al., 2014; Ielpi and Rainbird, 2016; Ielpi et al., 2017; Ghinassi and  
238 Ielpi, 2018).

239 Our results are not intended to exhaustively document all existing examples of  
240 meandering rivers developed in modern desert sedimentary basins, but rather to demonstrate  
241 that they are common features in environments where vegetation cover is limited. Whilst we  
242 acknowledge that rivers are dynamic systems that are subject to local climate and  
243 geomorphology, this study is solely dedicated to understanding planform development within the  
244 realm of desert sedimentary basins.

#### 245 4.2. Stabilization mechanisms in modern desert-basin rivers

246 Stabilization mechanisms for meander-belt development in the absence of vegetation  
247 include: (i) low-gradient alluvial plains, (ii) lateral confinement by aeolian dune-fields and dune

248 forms, and (iii) cohesion provided by salt and fine-grained sediments. According to our results  
249 (Table 1), 87% of meandering channels studied develop in endorheic basin settings in non- and  
250 poorly vegetated environments. Endorheic basins preserve all sedimentary material supplied to  
251 the basin (Nichols, 2007), particularly fine-grained sediments, which would otherwise bypass the  
252 fluvial system and be transported downstream into a shoreline realm, chiefly as suspended load  
253 (e.g., Walsh and Nittrouer, 2009). Additionally, endorheic desert basins are prone to evaporite  
254 precipitation and accumulation (Schütt, 1998), which can provide a surface and channel banks  
255 that are highly stabilized, as illustrated by the examples from the Bolivian Altiplano and the  
256 Amargosa River in Death Valley (Ielpi, 2019). Here we also note that one of the most spectacular  
257 examples of an endorheic basin meandering systems is the currently inactive Uzboy Channel  
258 (Karakum Desert, Turkmenistan), which preserves channels formed under an arid palaeoclimate  
259 from the Upper Pliocene to Preglacial Quaternary (Fet and Atamuradov, 1994; Létolle et al.,  
260 2007). However, the Uzboy channel is excluded from analysis herein since it is not possible to  
261 estimate the vegetation content for when this system was active.

262         The only studied examples of desert meandering rivers developed in exorheic basins (i.e.,  
263 Senegal River and the Inner Niger Delta; see discussions below) are characterized by fluvial-  
264 aeolian interactions. Wind-blown dust from the dune fields surrounding these meander-belts  
265 may also provide fine-grained sediments (e.g. Qiang et al., 2014) that serve to provide cohesion  
266 and stability to river channel banks in desert environments. Additionally, the Inner Niger Delta  
267 and Senegal River are two of the three lowest gradient systems in our studied examples.  
268 Importantly, the rivers in the present analysis are characterized by geomorphic features that are  
269 markedly different from most models of prevegetation rivers (e.g., the wide and shallow braided  
270 channels predicted by Cotter (1978). These examples are important in the construction of new  
271 models for prevegetation fluvial deposits.

272 The Senegal River meander belt (Fig. 2A) is restricted laterally by aeolian dune fields.  
273 Dune crests are oriented perpendicular to the trend of the meander belt, the transition being  
274 delineated by a sharp boundary typical of such fluvial-aeolian interaction (cf. Al-Masrahy and  
275 Mountney, 2015). This geomorphic style can commonly lead to mudstone and/or evaporitic  
276 sediment accumulation through floodwaters ponding against the edges of the adjoining aeolian  
277 dune fields (e.g. Stanistreet and Stollhofen, 2002). The reworking of such mudstone and  
278 evaporitic sediment could assist in promoting a cohesive lining to channel banks in desert  
279 meandering rivers. This is likely to be the case in the Senegal River; although fieldwork is needed  
280 to assess this hypothesis. The lateral relationship of the Senegal River to the non-vegetated dune  
281 fields to the north and south may promote meandering channel development through: (i) lateral  
282 confinement of the meander belt, and (ii) constant supply of sediment through dune-field  
283 erosion (Fig. 3D), both acting to restrict channel widening, and thus the change to a braided  
284 planform (e.g., Peakall et al., 2007).

285 The Senegal River also demonstrates that discharge variations, and related presence of  
286 vegetation, in desert environments do not necessarily impact river characteristics such as bankfull  
287 width and development of cutoff channels. Vegetation density increases significantly during the  
288 summer months (Fig. 9A); even during this period of relative drought relative to the wetter  
289 winter season (Fig. 9B); no changes in fluvial dynamics is observable between those periods. This  
290 increase in vegetation also hints at the opportunism of vegetation in occupying specific  
291 geomorphic niches. The described differences in water input during summer and winter likely  
292 result from the river being fed by areas external to the basin, providing perennial supply of water  
293 to the system.

294 Both the Senegal River and the Inner Niger Delta are characterized by more than one  
295 channel, each of which have individual meandering channel planforms. Whereas the Senegal  
296 River meander-belt is single and relatively rectilinear, the Inner Niger Delta is characterized by

297 multiple meander belts (Fig. 3B). These belts are mostly oriented parallel to surrounding aeolian  
298 dune forms, a situation which would promote the winnowing of fine-grained sediment (cf. Al-  
299 Masrahy and Mountney, 2015). This river not only records the development of an anabranching  
300 system in a poorly-vegetated environment, but also shows that such anabranches can individually  
301 develop a sinuous channel planform even when laterally restricted by rectilinear dunes and with  
302 banks that are therefore likely composed of a substantial proportion of matrix-free cohesionless  
303 sand reworked from adjacent aeolian dunes (Fig. 5E).

#### 304 4.3. Distribution of meandering rivers and vegetation in modern sedimentary basins

305 The presence of vegetation in the studied fluvial systems is concentrated in low-lying  
306 areas of the alluvial plain such as scroll bars and swales (e.g. Nanson, 1980; Mertes et al., 1995;  
307 Tooth et al., 2008), features resulting from point-bar deposition and which are prone to water  
308 stagnation and associated fine-grained sediment accumulation (e.g., Page et al., 2003). Muddy  
309 substrates typically encourage riverine plant growth (Prauová et al., 2015). This demonstrates  
310 the opportunism of vegetation in occupying specific geomorphic niches, as opposed to it acting  
311 as a geoengineer (cf. Corenblit et al., 2015). Vegetation requires sufficient humidity to prosper,  
312 but, as seen in the documented examples, the development of meandering channels can be  
313 achieved without vegetation.

314 It is likely that the meandering nature of the studied examples is the result of autogenic  
315 modulations that have an impact greater than that of vegetation (Erkens et al., 2011), particularly  
316 in tectonically active environments where an exogenic variable such as vegetation exerts less  
317 influence than a combination of processes related to dynamic equilibrium forms (Nanson and  
318 Huang, 2018). Those modulations include river self-organization through erosional and  
319 depositional processes (Stølum, 1996), which may have been influenced by river-bank cohesion  
320 (Peakall et al., 2007), induced by fine-grained deposition through small variations in flow depth  
321 (Howard, 2009). Such variations are supported by the analysis of multi-temporal imagery, which

322 show little oscillation in river flow and slow channel lateral migration (see Supplementary  
323 information for details), likely to be linked with low water input.

#### 324 4.4. Implications for rivers developed before land plant evolution

325         The majority (14 out of 16) of the examples documented here developed in endorheic  
326 basins (Table 1). This is a situation that likely increased the proportion of available fine-grained  
327 sediments compared to that in exorheic basins (e.g. Nichols, 2007). This may indicate that  
328 prevegetation river systems developed in such basin settings were more likely to develop  
329 meandering channel planforms than those developed on exorheic basins. The ability for  
330 prevegetation rivers to meander has also been credited to increased cohesion due to the presence  
331 of fine (Santos and Owen, 2016) and evaporitic sediments (Ielpi, 2019). Regarding the role of  
332 fine-grained sediment as an agent that promotes cohesion and strengthening of channel banks,  
333 the Helmand River (Afghanistan; this study) is currently incising Neogene deposits composed of,  
334 lacustrine silt and clay, and associated fluvial aeolian deposits. A similar situation occurs in the  
335 examples from Chad, which flow onto the exposed floor of the shrinking Lake Chad. These  
336 examples are similar to those described by Matsubara et al. (2015) as analogues to fluvial deposits  
337 on Mars.

338         Floodplain roughness is an additional variable which can induce sinuous channel  
339 development (Lazarus and Constantine, 2013); in desert basins this may result from the presence  
340 of aeolian bedforms. Non-vegetated, well-established aeolian dune fields commonly dominate  
341 the environments surrounding the studied meander belts (10 out of 16 examples). They are  
342 commonly topographically higher than the studied meander-belts and laterally constrain the  
343 fluvial systems (e.g., Senegal River), potentially countering lateral erosion through the near-  
344 continuous input of aeolian material, and hindering channel-widening and consequent evolution  
345 to a braided pattern (e.g., Schumm et al., 1987; Parker, 1998 ). Widespread aeolian dunes are also  
346 likely to have commonly occurred in barren, prevegetation fluvial systems (Long, 2011). Alluvial

347 slope and sediment types alone (Peakall et al., 2007; Van Dijk et al., 2013) appear to be  
348 insufficient to induce channel meandering, and our observations show a weak correlation  
349 between alluvial gradient and sinuosity. These results differ from numerical models on the  
350 behaviour of prevegetation low-gradient areas, which predict that such rivers should be braided  
351 (Almeida et al., 2016).

352 In the majority of examples, meandering rivers form the dominant fluvial planform over  
353 much of the central parts of the studied basins. This suggests that prevegetation fluvial systems  
354 could develop meandering systems in the central parts of the basin. The sparseness of crevasse  
355 splays in our examples is likely an indication that avulsion frequency is lower in these systems,  
356 this being mostly the result of water sparseness in deserts; a characteristic not necessarily  
357 applicable to the prevegetation rock record.

358 Schemes that classify river morphology into end-members may be simplistic (Bridge,  
359 1993; Ethridge, 2011) but they persist in the literature and are widely applied. Although  
360 interpretations of braided fluvial systems of all geological ages are dominant and far more  
361 abundant than those of meandering systems in the published literature (Gibling, 2006;  
362 Colombera et al., 2013), a large proportion (~46%) of distributive fluvial systems developed in  
363 modern sedimentary basins, including dryland areas, develop sinuous channel planforms (Hartley  
364 et al., 2015). Such an observation suggests that many sandy meander-belt deposits may not have  
365 been identified correctly in the fluvial rock record (e.g. Swan et al., 2019) and may also imply that  
366 amalgamated meandering sandy fluvial systems could be under-represented in pre-Devonian  
367 fluvial deposits. Our observations suggest that prevegetation meandering rivers may have been  
368 more common than previously envisaged, and the examples described here are potential  
369 analogues for prevegetation fluvial deposits (Santos and Owen, 2016).

## 370 **5. Conclusions**

371 Remotely sensed imagery shows that terrestrial meandering rivers can form where  
372 vegetation is restricted or absent. Crevasse splays are rare in non- and poorly-vegetated settings,  
373 and floodplain settings are commonly dominated by aeolian processes. Most examples of  
374 meandering rivers in desert basins are related to major drainage systems of their respective  
375 basins. By contrast, braided channels tend to be related to smaller-scale drainages and  
376 catchments. Stabilization mechanisms in the absence of vegetation include cohesion provided by  
377 fine-grained sediments and salt, and constant sediment input from adjacent aeolian dune fields.  
378 Endorheic basin settings are more likely to preserve meandering channel deposits in non- and  
379 poorly vegetated environments. These systems may make excellent analogues for prevegetation  
380 systems, yet are characterized by geomorphic features that are markedly different (i.e., narrow  
381 and single, meandering channels) from current models of prevegetation rivers.

### 382 **Acknowledgements.**

383 We thank Reviewer Massimiliano Ghinassi and an anonymous reviewer, and also Editor Jasper  
384 Knight for their helpful comments and suggestions, which have significantly improved the  
385 manuscript. M.G.M.S. was supported by grant #2014/13937-3, São Paulo Research Foundation  
386 (FAPESP).

387

### 388 **References**

- 389 Al-Masrahy, M.A., Mountney, N.P., 2015. A classification scheme for fluvial–aeolian system  
390 interaction in desert-margin settings. *Aeolian Research* 17, 67–88.
- 391 Almeida, R.P., Marconato, A., Freitas, B., Tura, B.B., 2016. The ancestors of meandering rivers.  
392 *Geology* 44, 203–206.
- 393 Billi, P., Demissie, B., Nyssen, J., Moges, G., Fazzini, M., 2018. Meander hydromorphology of  
394 ephemeral streams: Similarities and differences with perennial rivers. *Geomorphology* 319,

395 35–46.

396 Braudrick, C.A., Dietrich, W.E., Leverich, G.T., Sklar, L.S., 2009. Experimental evidence for the  
397 conditions necessary to sustain meandering in coarse-bedded rivers. *Proceedings of the*  
398 *National Academy of Sciences* 106, 16936–16941.

399 Bridge, J.S., 1993. Description and interpretation of fluvial deposits: a critical perspective.  
400 *Sedimentology* 40, 801–810.

401 Burr, D.M., Taylor Perron, J., Lamb, M.P., Irwin, R.P., Collins, G.C., Howard, A.D., Sklar, L.S.,  
402 Moore, J.M., Ádámkóvics, M., Baker, V.R., Drummond, S.A., Black, B.A., 2013. Fluvial  
403 features on Titan: Insights from morphology and modeling. *Bulletin of the Geological*  
404 *Society of America* 125, 299–321.

405 Colombera, L., Mountney, N.P., McCaffrey, W.D., 2013. A quantitative approach to fluvial facies  
406 models: Methods and example results. *Sedimentology* 60, 1526–1558.

407 Corenblit, D., Davies, N.S., Steiger, J., Gibling, M.R., Bornette, G., 2015. Considering river  
408 structure and stability in the light of evolution: Feedbacks between riparian vegetation and  
409 hydrogeomorphology. *Earth Surface Processes and Landforms* 40, 189–207.

410 Cotter, E., 1978. The evolution of fluvial style, with special reference to the central Appalachian  
411 Palaeozoic. In: Miall, A.D. (Ed.), *Fluvial Sedimentology*, Canadian Society of Petroleum  
412 Geologists Memoir pp. 361–384.

413 Davies, N.S., Gibling, M.R., 2010. Cambrian to Devonian evolution of alluvial systems: The  
414 sedimentological impact of the earliest land plants. *Earth-Science Reviews* 98, 171–200.

415 Davies, N.S., Gibling, M.R., McMahon, W.J., Slater, B.J., Long, D.G.F., Bashforth, A.R., Berry,  
416 C.M., Falcon-Lang, H.J., Gupta, S., Rygel, M.C., Wellman, C.H., 2017. Discussion on  
417 ‘Tectonic and environmental controls on Palaeozoic fluvial environments: reassessing the

418 impacts of early land plants on sedimentation'. *Journal of the Geological Society* 174, 947-  
419 950.

420 Eriksson, P.G., Bumby, A.J., Brüner, J.J., Neut, M., 2006. Precambrian fluvial deposits:  
421 Enigmatic palaeohydrological data from the c. 2-1.9 Ga Waterberg Group, South Africa.  
422 *Sedimentary Geol.* 190, 25–46.

423 Erkens, G., Hoffmann, T., Gerlach, R., Klostermann, J., 2011. Complex fluvial response to  
424 Lateglacial and Holocene allogenic forcing in the Lower Rhine Valley (Germany).  
425 *Quaternary Science Reviews* 30, 611–627.

426 ESRI, 2013. *ArcGIS Desktop: Release 10.2*. Redlands CA.

427 Ethridge, F.G., 2011. Interpretation of ancient fluvial channel deposits: Review and  
428 recommendations. *From River to Rock Record: The preservation of fluvial sediments and*  
429 *their subsequent interpretation*. In: Davidson, S.K., Leleu, S., North, C. (Eds.), *From River*  
430 *to Rock Record: The Preservation of Fluvial Sediments and their Subsequent Interpretation:*  
431 *SEPM Spec. Publ.*, 97, pp. 9–36.

432 Fet, V., Atamuradov, K., 1994. *Biogeography and Ecology of Turkmenistan*. Kluwer, Dordrecht.

433 Funk, C., Peterson, P., Landsfeld, M., Pedreros, D., Verdin, J., Shukla, S., Husak, G., Rowland, J.,  
434 Harrison, L., Hoell, A., Michaelsen, J., 2015. The climate hazards infrared precipitation with  
435 stations—a new environmental record for monitoring extremes. *Scientific Data*, 2, 150066.  
436 [10.1038/sdata.2015.66](https://doi.org/10.1038/sdata.2015.66).

437 Ghinassi, M. and Ielpi, A. (2018), Precambrian snapshots: Morphodynamics of Torridonian  
438 fluvial braid bars revealed by three-dimensional photogrammetry and outcrop  
439 sedimentology. *Sedimentology* 65, 492-516.

440 Gibling, M.R., 2006. Width and Thickness of Fluvial Channel Bodies and Valley Fills in the

441 Geological Record: A Literature Compilation and Classification. *Journal of Sedimentary*  
442 *Research* 76, 731–770.

443 Gorelick, N., Hancher, M., Dixon, M., Ilyushchenko, S., Thau, D., Moore, R., 2017. Google  
444 Earth Engine: Planetary-scale geospatial analysis for everyone. *Remote Sensing of*  
445 *Environment* 202, 18-27.

446 Hartley, A.J., Owen, A., Swan, A., Weissmann, G.S., Holzweber, B.I., Howell, J., Nichols, G.,  
447 Scuderi, L., 2015. Recognition and importance of amalgamated sandy meander belts in the  
448 continental rock record. *Geology* 43, 679–682.

449 Hirt, C., 2018. Artefact detection in global digital elevation models (DEMs): The maximum slope  
450 approach and its application for 1 complete screening of the SRTM v4.1 and MERIT  
451 DEMs. *Remote Sensing of Environment* 207, 27–41.

452 Howard, A.D., 2009. How to make a meandering river. *Proceedings of the National Academy of*  
453 *Sciences* 106, 17245–17246.

454 Ielpi, A., 2017a. Lateral accretion of modern unvegetated rivers: Remotely sensed fluvial-aeolian  
455 morphodynamics and perspectives on the Precambrian rock record. *Geological Magazine*  
456 154, 609–624.

457 Ielpi, A., 2017b. Controls on sinuosity in the sparsely vegetated Fossálar River, southern Iceland.  
458 *Geomorphology* 286, 93–109.

459 Ielpi, A., 2019. Morphodynamics of meandering streams devoid of plant life: Amargosa River ,  
460 Death Valley , California. *Bulletin of the Geological Society of America*, in press.

461 Ielpi, A., Rainbird, R.H, 2016. Highly variable Precambrian fluvial style recorded in the Nelson  
462 Head Formation of Brock Inlier (Northwest Territories, Canada). *Journal of Sedimentary*  
463 *Research* 86, 199–216.

464 Ielpi, A., Rainbird, R.H., Ventra, D., Ghinassi, M., 2017. Morphometric convergence between  
465 Proterozoic and post-vegetation rivers. *Nature Communications* 8, Article 15250. Jansen,  
466 J.D., Nanson, G.C., 2010. Functional relationships between vegetation, channel  
467 morphology, and flow efficiency in an alluvial (anabranching) river. *Journal of Geophysical*  
468 *Research: Earth Surface* 115, F04030.

469 Jarvis, A., H.I. Reuter, A. Nelson, E. Guevara, 2008, Hole-filled SRTM for the globe Version 4,  
470 available from the CGIAR-CSI SRTM 90m Database (<http://srtm.csi.cgiar.org>).

471 Kottek, M., Grieser, J., Beck, C., Rudolf, B., Rubel, F., 2006. World map of the Köppen-Geiger  
472 climate classification. *Meteorologische Zeitschrift* 15, 259–263.

473 Lazarus, E.D., Constantine, J.A., 2013. Generic theory for channel sinuosity. *Proceedings of the*  
474 *National Academy of Sciences* 110, 8447–8452.

475 Leopold, L.B., Wolman, M.G., Miller, J.P., 1964. *Fluvial processes in geomorphology*. Freeman,  
476 San Francisco, 522 p.

477 Létolle, R., Micklin, P., Aladin, N., Plotnikov, I., 2007. Uzboy and the Aral regressions: A  
478 hydrological approach. *Quat. Int.* 173–174, 125–136.

479 Li, J., Bristow, C.S., 2015. Crevasse splay morphodynamics in a dryland river terminus: Río  
480 Colorado in Salar de Uyuni Bolivia. *Quaternary International* 377, 71–82.

481 Li, J., Bristow, C.S., Luthi, S.M., Donselaar, M.E., 2015. Dryland anabranching river  
482 morphodynamics: Río Capilla, Salar de Uyuni, Bolivia. *Geomorphology* 250, 282–297.

483 Li, Z., Yu, G.A., Brierley, G.J., Wang, Z., Jia, Y., 2017. Migration and cutoff of meanders in the  
484 hyperarid environment of the middle Tarim River, northwestern China. *Geomorphology*  
485 276, 116–124.

486 Long, D.G.F., 1978. Proterozoic stream deposits: some problems of recognition and

487 interpretation of ancient sandy fluvial systems. In: Miall, A.D. (Ed.), *Fluvial Sedimentology*,  
488 Canadian Society of Petroleum Geologists Memoir, pp. 313–342.

489 Long, D.G.F., 2006. Architecture of pre-vegetation sandy-braided perennial and ephemeral river  
490 deposits in the Paleoproterozoic Athabasca Group, northern Saskatchewan, Canada as  
491 indicators of Precambrian fluvial style. *Sedimentary Geology* 190, 71–95.

492 Long, D.G.F., 2011. Architecture and Depositional Style of Fluvial Systems before Land Plants:  
493 A Comparison of Precambrian, Early Paleozoic, and Modern River Deposits. In: Davidson,  
494 S.K., Leleu, S., North, C. (Eds.), *From River to Rock Record: The Preservation of Fluvial*  
495 *Sediments and their Subsequent Interpretation: SEPM Spec. Publ.*, 97, pp. 37–61.

496 Matsubara, Y., Howard, A.D., Burr, D.M., Williams, R.M.E., Dietrich, W.E., Moore, J.M., 2015.  
497 River meandering on Earth and Mars: A comparative study of Aeolis Dorsa meanders, Mars  
498 and possible terrestrial analogs of the Usuktuk River, AK, and the Quinn River, NV.  
499 *Geomorphology* 240, 102–120.

500 McMahon, W.J., Davies, N.S., 2017. High-energy flood events recorded in the Mesoproterozoic  
501 Meall Dearg Formation, NW Scotland; their recognition and implications for the study of  
502 pre-vegetation alluvium. *Journal of the Geological Society* 175, 13–32.

503 McMahon, W.J., Davies, N.S., 2018. Evolution of alluvial mudrock forced by early land plants.  
504 *Science* 359, 1022–1024.

505 Mertes, L.A.K.; Daniel, D.L.; Melack, J.M.; Nelson, B.; Martinelli, L.A.; Forsberg, B.R., 1995.  
506 Spatial patterns of hydrology, geomorphology, and vegetation on the floodplain of the  
507 Amazon river in Brazil from a remote sensing perspective. *Geomorphology* 13, 215-232.

508 Nanson, G.C., Huang, H.Q., 2018. A philosophy of rivers: Equilibrium states, channel evolution,  
509 teleomatic change and least action principle. *Geomorphology* 302, 3–19.

- 510 Nichols G. 2007. Fluvial systems in desiccating endorheic basins. In: *Sedimentary Processes,*  
511 *Environments and Basins: A Tribute to Peter Friend*, Nichols G, Williams E, Paola C (eds).  
512 Blackwell Publishing: Oxford; 569–589.
- 513 Nyberg, B., Howell, J.A., 2015. Is the present the key to the past? A global characterization of  
514 modern sedimentary basins. *Geology* 43, 643–646.
- 515 Page, K. J., Nanson, G. C., Frazier, P. S., 2003. Floodplain formation and sediment stratigraphy  
516 resulting from oblique accretion on the Murrumbidgee River, Australia. *Journal of*  
517 *Sedimentary Research* 73, 5–14.
- 518 Parker, G., 1998. River meanders in a tray. *Nature* 395, 111–112.
- 519 Peakall, J., Ashworth, P.J., Best, J.L., 2007. Meander-bend evolution, alluvial architecture, and the  
520 role of cohesion in sinuous river channels: a flume study. *Journal of Sedimentary Research*  
521 77, 197–212.
- 522 Planet Team (2017). Planet Application Program Interface: In *Space for Life on Earth*. San  
523 Francisco, CA. <https://api.planet.com>.
- 524 Prausová, R., Kozelková, Z., Šafářová, L., 2015. Protocol for acclimatization of in vitro cultured  
525 *Potamogeton praelongus* – aspect of plantlet size and type of substrate. *Acta Societatis*  
526 *Botanicorum Poloniae* 84, 35–41.
- 527 Qiang, M., Liu, Y. Jin, Y., Song, L., Huang, X., Chen, F. (2014), Holocene record of eolian  
528 activity from Genggahai Lake, northeastern Qinghai-Tibetan Plateau, China, *Geophysical*  
529 *Research Letters* 41, 589–595.
- 530 Rodriguez, E., Morris, C.S., Belz, J., Chapin, E., Martin, J., Daffer, W., Hensley, S., 2005. An  
531 Assessment of the SRTM Topographic Products, Technical Report JPL D-31639, Jet  
532 Propulsion Laboratory, Pasadena, California.

533 Santos, M.G.M., Owen, G., 2016. Heterolithic meandering-channel deposits from the  
534 Neoproterozoic of NW Scotland: Implications for palaeogeographic reconstructions of  
535 Precambrian sedimentary environments. *Precambrian Research* 272, 226–243.

536 Santos, M.G.M., Almeida, R.P., Godinho, L.P.S., Marconato, A., Mountney, N.P., 2014. Distinct  
537 styles of fluvial deposition in a Cambrian rift basin. *Sedimentology* 61, 881-914.

538 Santos, M.G.M., Mountney, N.P., Peakall, J., 2017a. Tectonic and environmental controls on  
539 palaeozoic fluvial environments: Reassessing the impacts of early land plants on  
540 sedimentation. *Journal of the Geological Society* 174, 393-404.

541 Santos, M.G.M., Mountney, N.P., Peakall, J., Thomas, R.E., Wignall, P.B., Hodgson, D.M.,  
542 2017b. Reply to Discussion on ‘Tectonic and environmental controls on Palaeozoic fluvial  
543 environments: Reassessing the impacts of early land plants on sedimentation’ *Journal of the*  
544 *Geological Society* 174, 950-952.

545 Schon, S.C., Head, J.W., Fassett, C.I., 2012. An overfilled lacustrine system and progradational  
546 delta in Jezero crater, Mars: Implications for Noachian climate. *Planetary and Space Science*  
547 67, 28–45.

548 Schumm, S.A., 1968. Speculations concerning paleohydrologic controls of terrestrial  
549 sedimentation. *Bulletin of the Geological Society of America* 79, 1573–1588.

550 Schumm, S.A., Mosley, M.P., Weaver, W.E., 1987. *Experimental Fluvial Geomorphology*. John  
551 Wiley & Sons, New York.

552 Schütt, B. 1998. Reconstruction of palaeoenvironmental conditions by investigation of Holocene  
553 playa sediments in the Ebro Basin, Spain: preliminary results. *Geomorphology* 23, 273–283.

554 Sønderholm, M., Tirsgaard, H., 1998. Proterozoic fluvial styles: Responses to changes in  
555 accommodation space (Rivieradal sandstones, eastern North Greenland). *Sedimentary*

556 Geology 120, 257–274.

557 Stanistreet, I.G., Stollhofen, H., 2002. Hoanib River flood deposits of Namib Desert interdunes  
558 as analogues for thin permeability barrier mudstone layers in aeolianite reservoirs.  
559 Sedimentology 49, 719–736.

560 Stølum, H.H., 1996. River meandering as a self-organization process. Science 271, 1710–1713.

561 Swan, A., Hartley, A.J., Owen, A., and Howell, J. 2019. Reconstruction of a sandy point-bar  
562 deposit: implication for fluvial facies analysis. In: Ghinassi, M., Colombera, L., Mountney,  
563 N.P., and Reeskink, A.J.H. Fluvial Meanders and Their Sedimentary Products in the Rock  
564 Record. International Association of Sedimentology special publication 48, 445-508.

565 Tal, M., Paola, C., 2010. Effects of vegetation on channel morphodynamics: Results and insights  
566 from laboratory experiments. Earth Surface Processes and Landforms 35, 1014–1028.

567 Tooth, S., 2000. Process, form and change in dryland rivers: a review of recent research. Earth-  
568 Science Reviews 51, 67–107.

569 Tooth, S., Jansen, J., Nanson, G., Coulthard, T., Pietsch, T., 2008. Riparian vegetation and the  
570 late Holocene development of an anabranching river: Magela Creek, northern Australia.  
571 Geological Society of America Bulletin 120, 1212–1224.

572 Van de Lageweg, W.I., van Dijk, W.M., Baar, A.W., Rutten, J., Kleinhans, M.G., 2014. Bank pull  
573 or bar push: What drives scroll-bar formation in meandering rivers? Geology 42, 319–322.

574 Van Dijk, W.M., Van de Lageweg, W.I., Kleinhans, M.G., 2013. Formation of a cohesive  
575 floodplain in a dynamic experimental meandering river. Earth Surface Processes and  
576 Landforms 38, 1550–1565.

577 Vogt, T., 1941. Geology of a Middle Devonian cannel coal from Spitsbergen. Norwegian Journal  
578 of Geology 21, 1-12.

- 579 Walsh, J.P., Nittrouer, C.A., 2009. Understanding fine-grained river-sediment dispersal on  
580 continental margins. *Marine Geology* 263, 34–45.
- 581 Went, D.J., McMahon, W.J., 2018. Fluvial products and processes before the evolution of land  
582 plants: Evidence from the lower Cambrian Series Rouge, English Channel region.  
583 *Sedimentology* 65, 2559-2594.
- 584 Wolman, M.G., Brush, L.M., 1961. Factors controlling the size and shape of stream channels in  
585 coarse non-cohesive sands. United States Geological Survey Professional Paper 282-G, 183–  
586 210.
- 587

588 **FIGURE AND TABLE CAPTIONS**

589

590 **Fig. 1.** Global map featuring poorly to non-vegetated meandering rivers (circles) developed in  
591 modern desert basins (adapted from Nyberg and Howell, 2015): 1 – Algeria; 2 – Southern  
592 Altiplano Plateau, Bolivia; 3 – Amargosa River, Death Valley, USA; 4 – Batha River, Chad; 5 –  
593 Bermejo River, Argentina; 6 – Ephemeral river in Chad; 7 – Helmand River, Afghanistan; 8 –  
594 Inner Niger Delta, Mali; 9 – ephemeral river in Niger; 10 – Senegal River, Senegal/Mauritania; 11  
595 – Taklamakan Desert river 1, China; 12 – Taklamakan Desert river 2, China; 13 – river in Ak-  
596 Altyn, Turkmenistan; 14 – Warburton River, Australia; 15 – Yobe River, Nigeria; 16 –  
597 Zhanadarya River, Kazakhstan.

598

599 **Fig. 2.** Examples of vegetation cover classification, highlighting (left), in yellow, the limits of  
600 selected meander belt areas and (right) resulting vegetation aerial identification. (A) Senegal  
601 River. (B) Zhanadarya River. (C) Unnamed ephemeral river in Chad. See supplementary data for  
602 all the classified examples. Black arrows at upper right of each image indicate river-flow  
603 direction.

604

605 **Fig. 3.** Selected examples of poorly and non-vegetated meandering rivers. (A) Oxbow lakes in  
606 the Zhanadarya River, Kazakhstan. (B) Aeolian linear dunes and scrolls in the Inner Niger  
607 Delta, Mali. (C) Crevasse-splay and channel cutoff in the Warburton River, Australia. (D)  
608 Laterally-eroding channels, scrolls and aeolian dunes in the Senegal River, Senegal/Mauritania.  
609 Black arrows at upper right of each image indicate river-flow direction.

610

611 **Fig. 4.** Detailed view of selected poorly- to non-vegetated meandering rivers. (A) Scrolls and  
612 abandoned channel form preserved of an ephemeral river in the Tarim Basin, China. (B) Scrolls

613 and abandoned channel form of an unnamed ephemeral river in the Sahara Desert in Chad. (C)  
614 Channel cutoff and valley limits of the Helmand River, Afghanistan. (D) Bermejo River,  
615 Argentina. Black arrows at upper right of each image indicates river-flow direction.

616

617 **Fig. 5.** Inner Niger Delta, Mali. (A) General view of the Inner Niger Delta as it crosses the  
618 southern Sahara Desert. (B) Detail of (A) showing the trunk system (arrow) and two  
619 anabranches with meandering planform. (C) Detail showing anabranches splitting into smaller  
620 channels (arrow). (D) Detail of much smaller channel (see location on C). (E) Small channel  
621 (arrow) flowing between linear aeolian dunes. Black bar (upper right) is 50 km.

622

623 **Fig. 6.** Warburton River in Simpson Desert (Lake Eyre, Australia). (A) General view of the  
624 Warburton River. (B) Crevasse development into floodplain lake. (C) Detail of the Warburton  
625 River channel entrenched into surrounding areas. (D) Development of scroll features. (E)  
626 Channel cut-off development. Black bar is 20 km long.

627

628 **Fig. 7.** Graph of sinuosity against (A) percentage of meander belt vegetation cover, (B)  
629 vegetation cover of areas surrounding studied meander belts, (C) total area of alluvial plain  
630 vegetation cover and (D) alluvial plain gradient for the studied rivers.

631

632 **Fig. 8.** Examples of agents and mechanisms acting to provide cohesion other than vegetation.  
633 Evaporitic floodplain sediments providing channel-bank cohesion (A) Uyuni Desert, Bolivia, and  
634 (B) Amargosa River, Death Valley. Fine-grained sandy and silty material: (C) ephemeral tributary  
635 of the Tarim River, China.

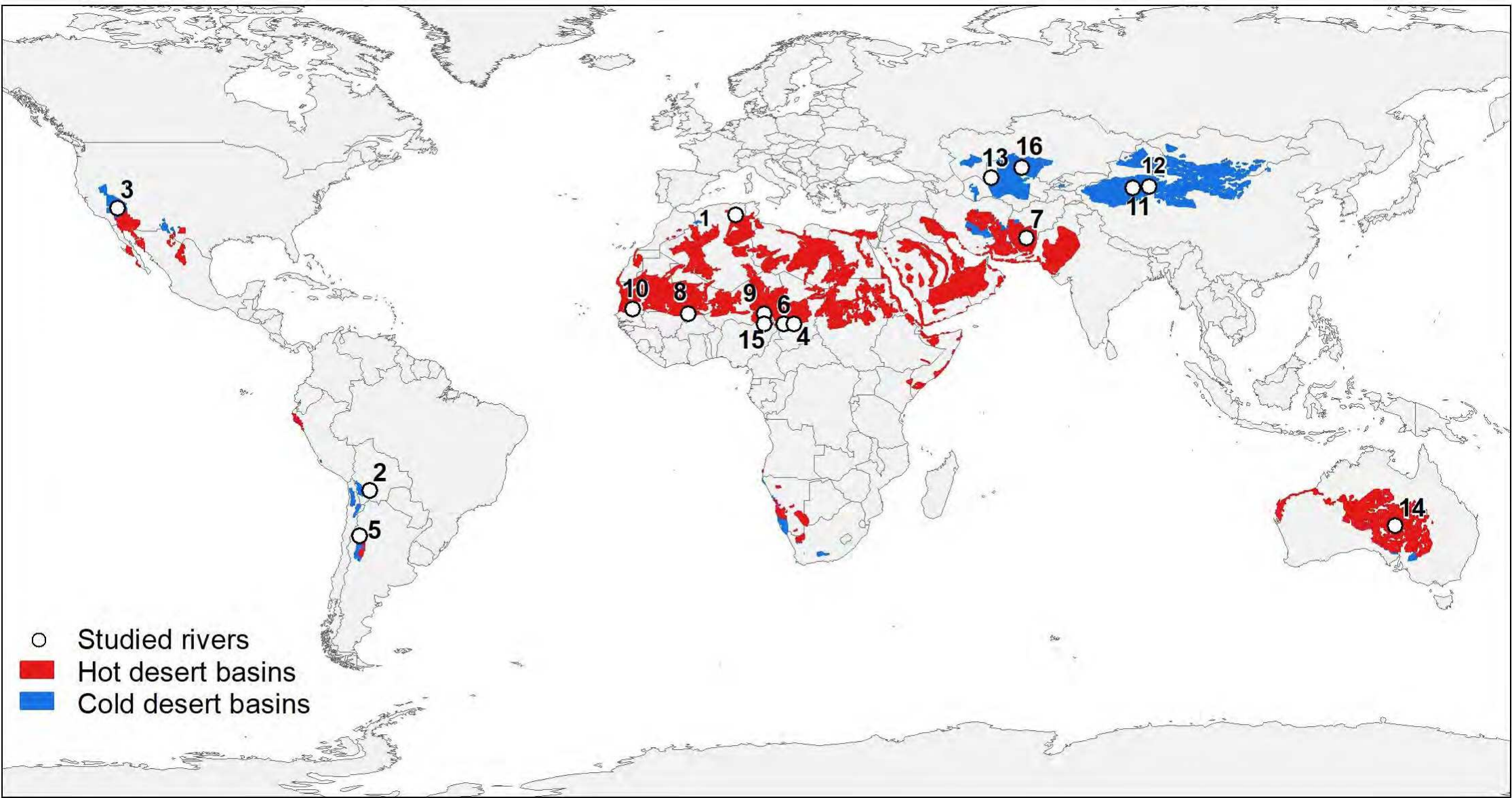
636

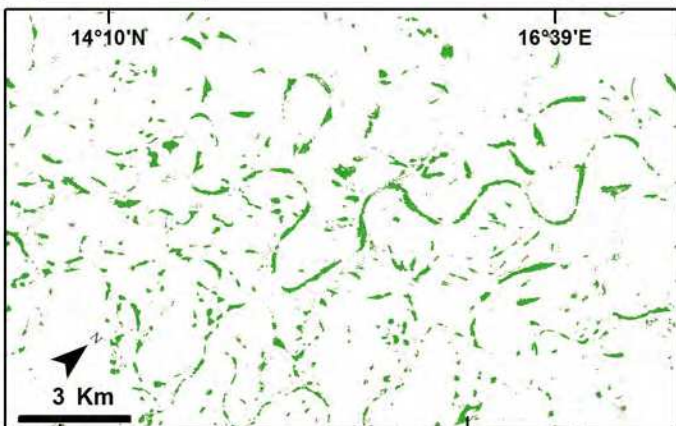
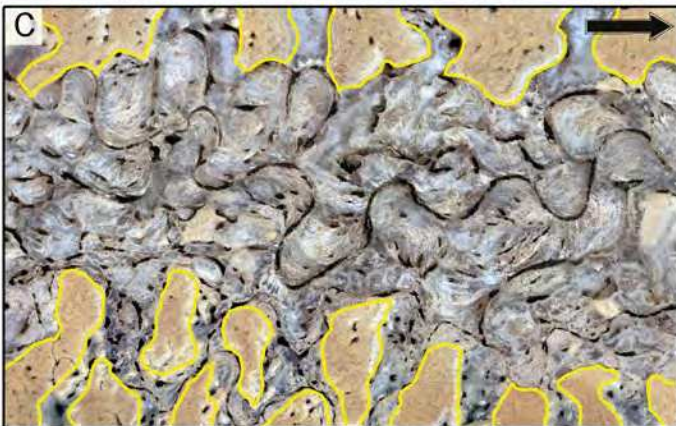
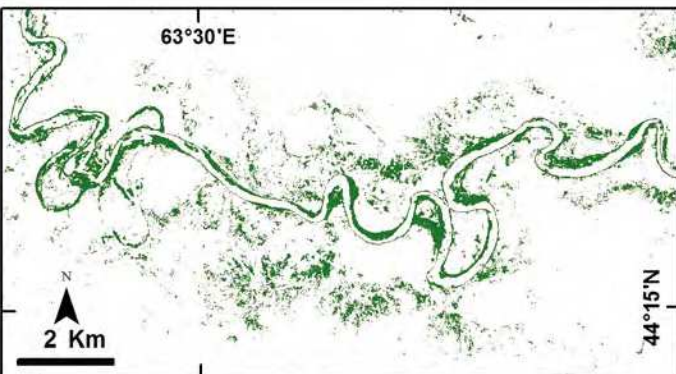
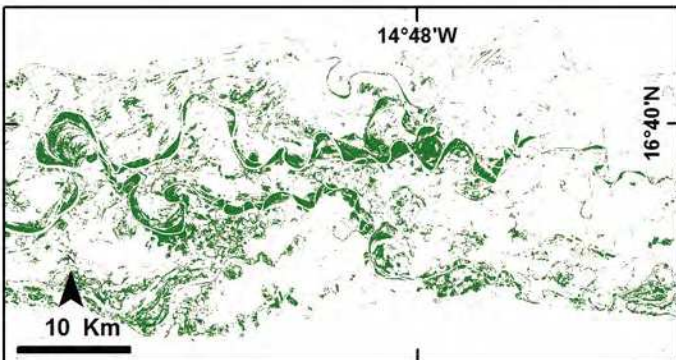
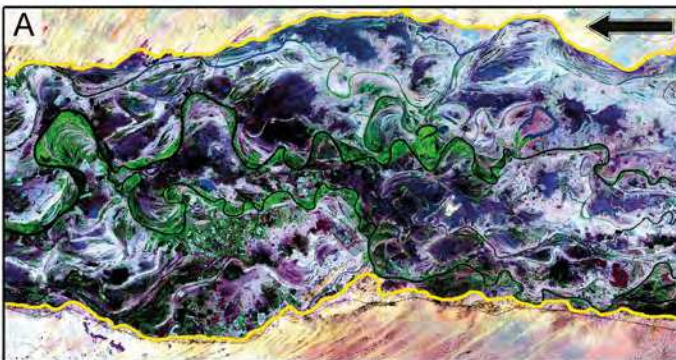
637 **Fig. 9.** Wet and dry seasons at the Senegal River (Senegal/Mauritania). One-month mosaic of  
638 Planet Images showing vegetation cover differences between (A) dry season and (B) wet season  
639 can be observed. Insert (lower right): CHIRPS climogram depicting temperature and rainfall at  
640 the region (average of last 30 years for rainfall and last 20 years for temperature).

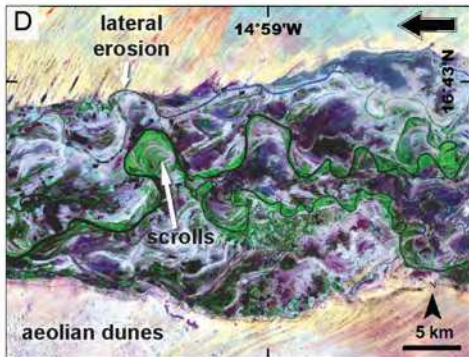
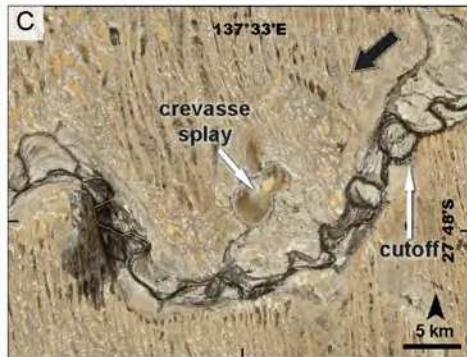
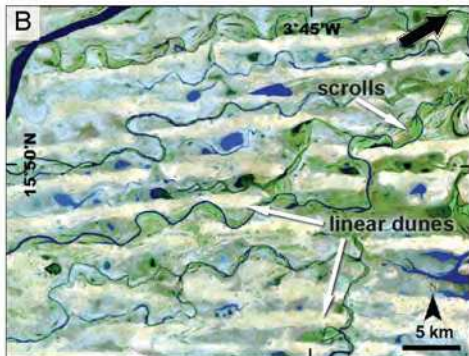
641

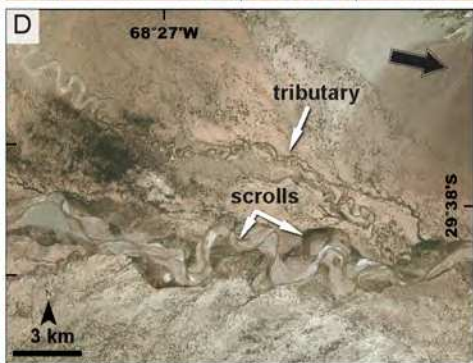
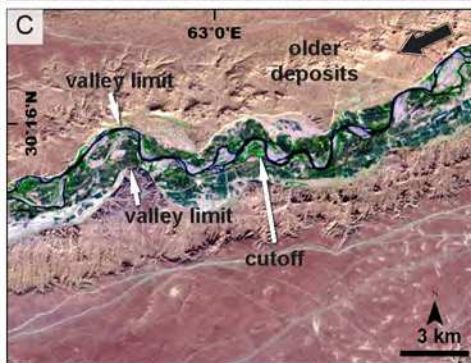
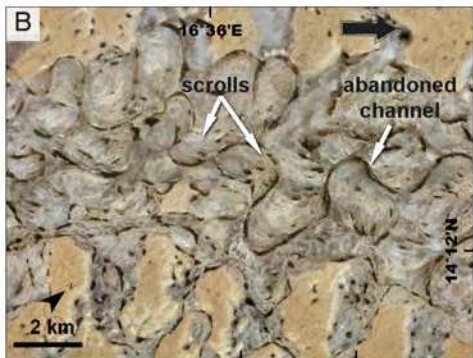
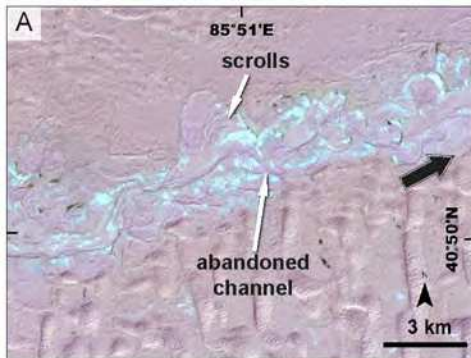
642 **Table 1** Morphometric data of the studied rivers.

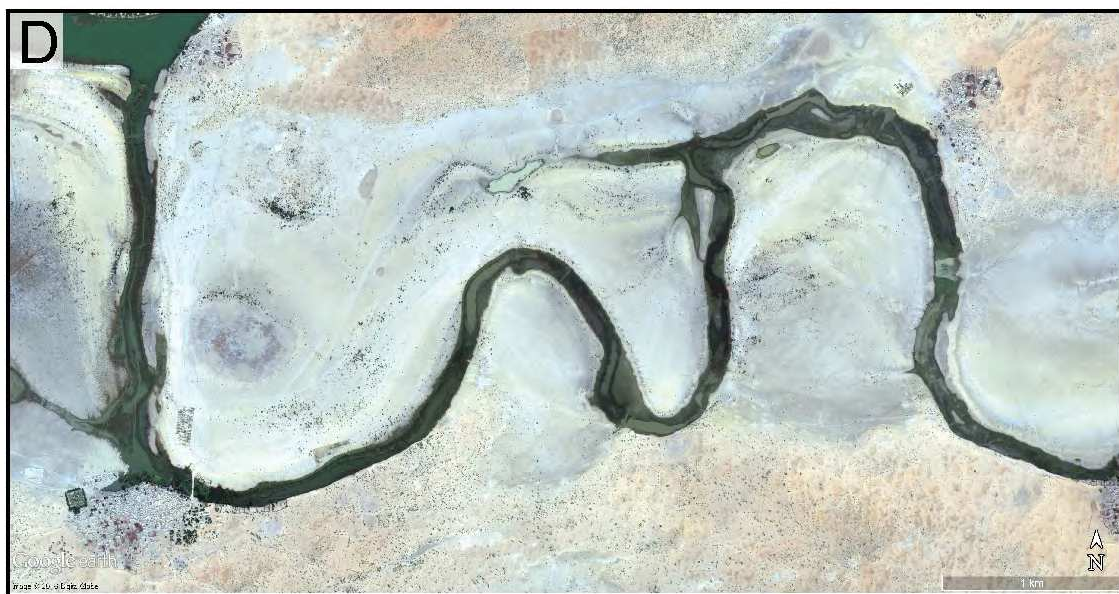
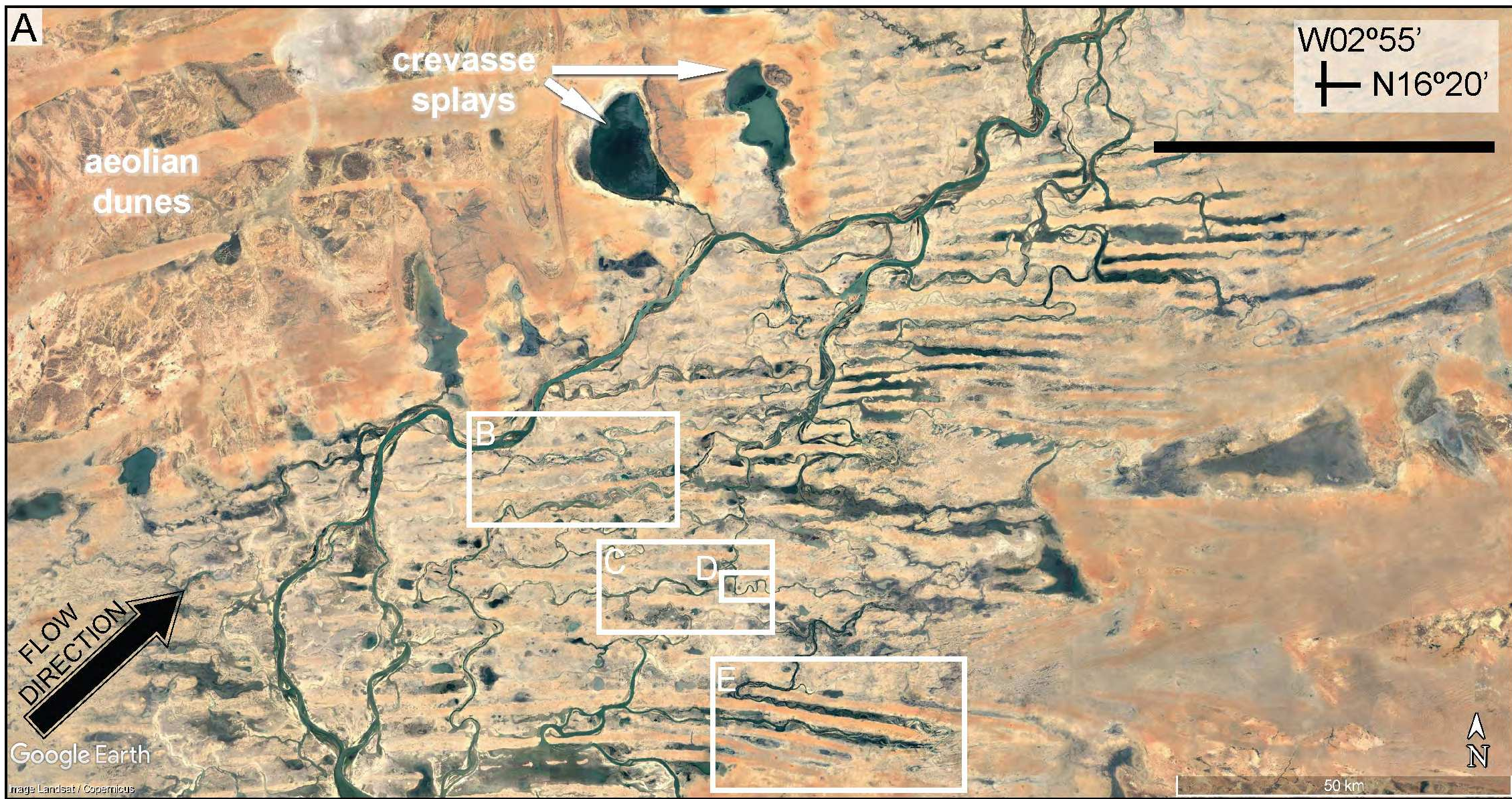
643

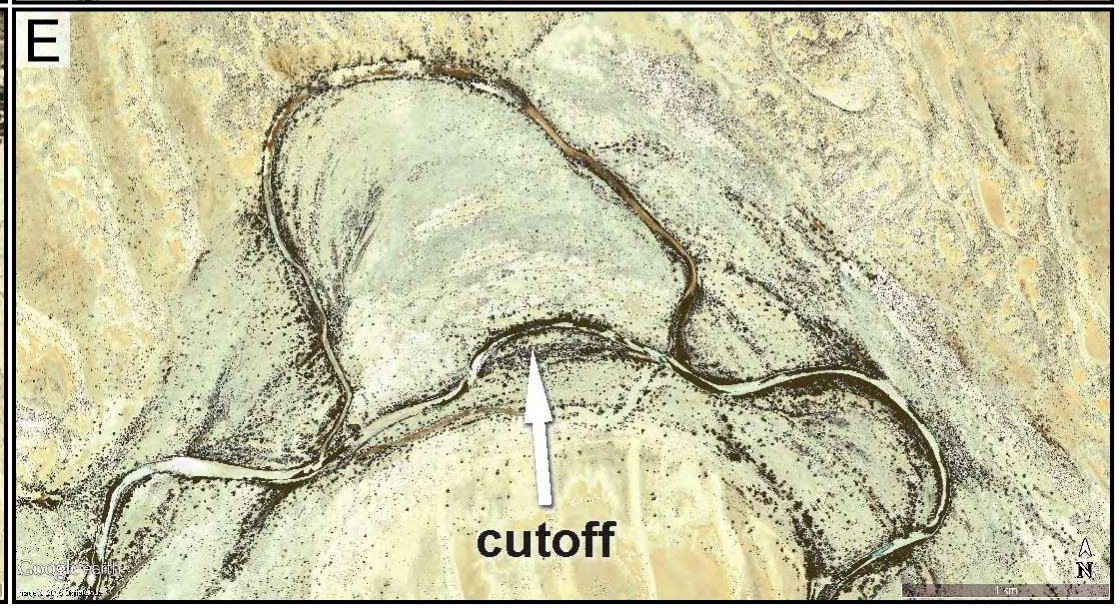
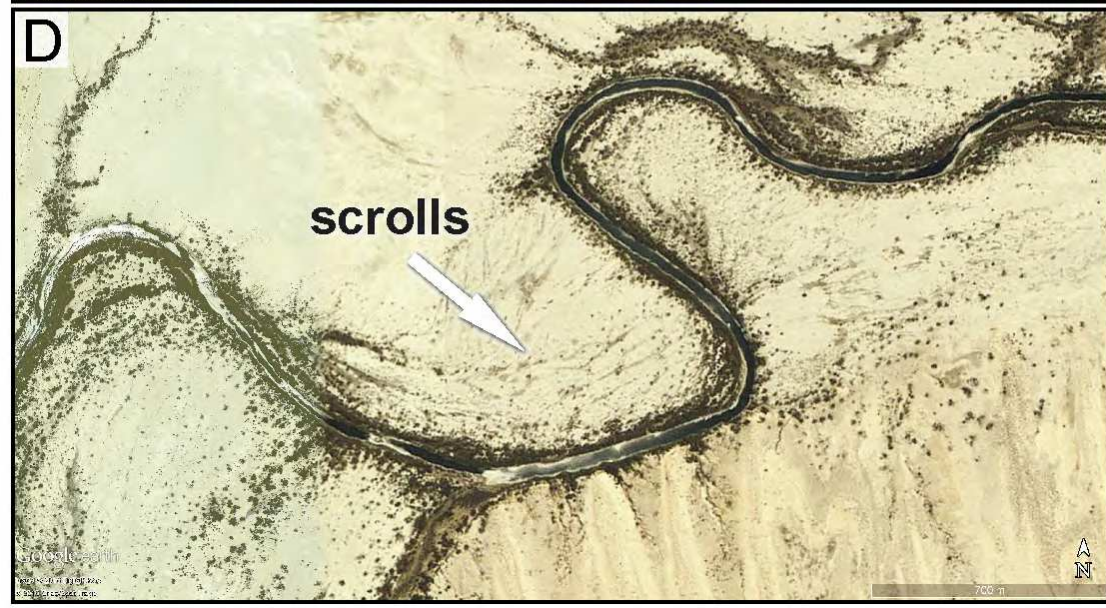
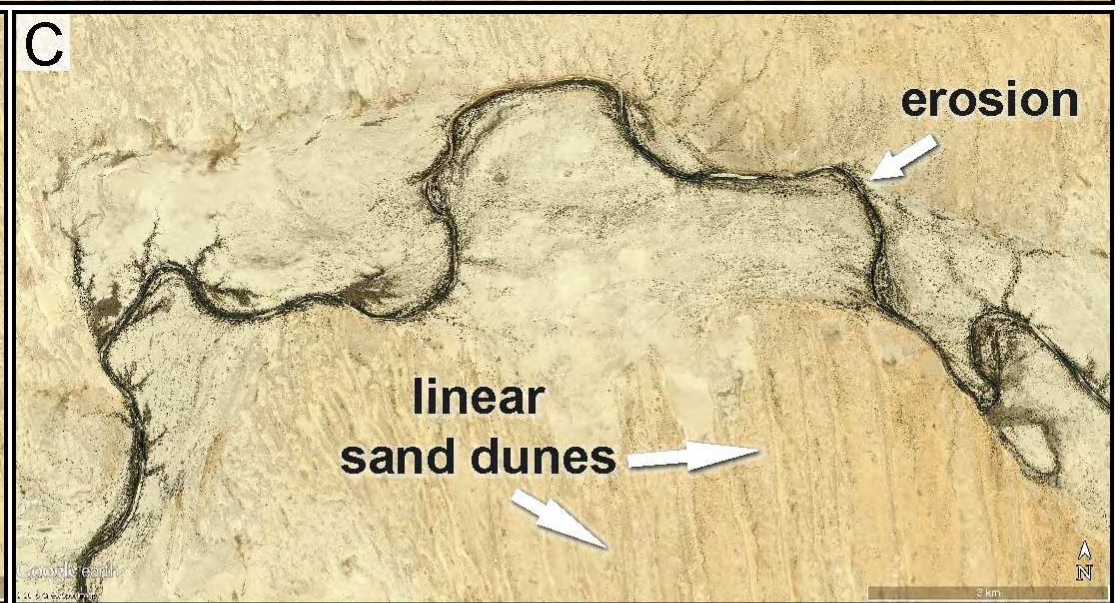
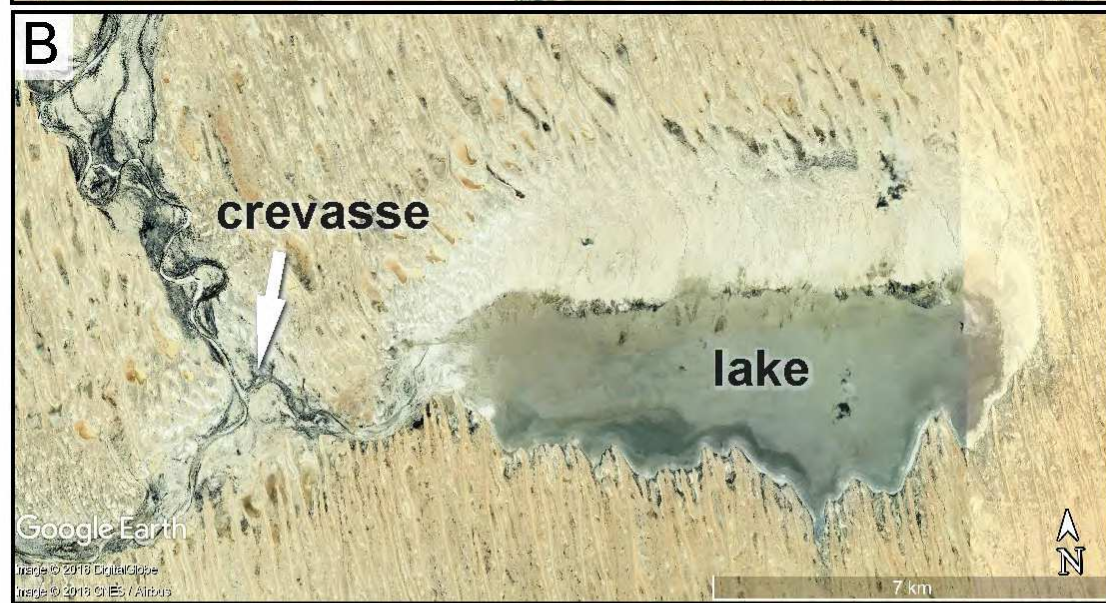


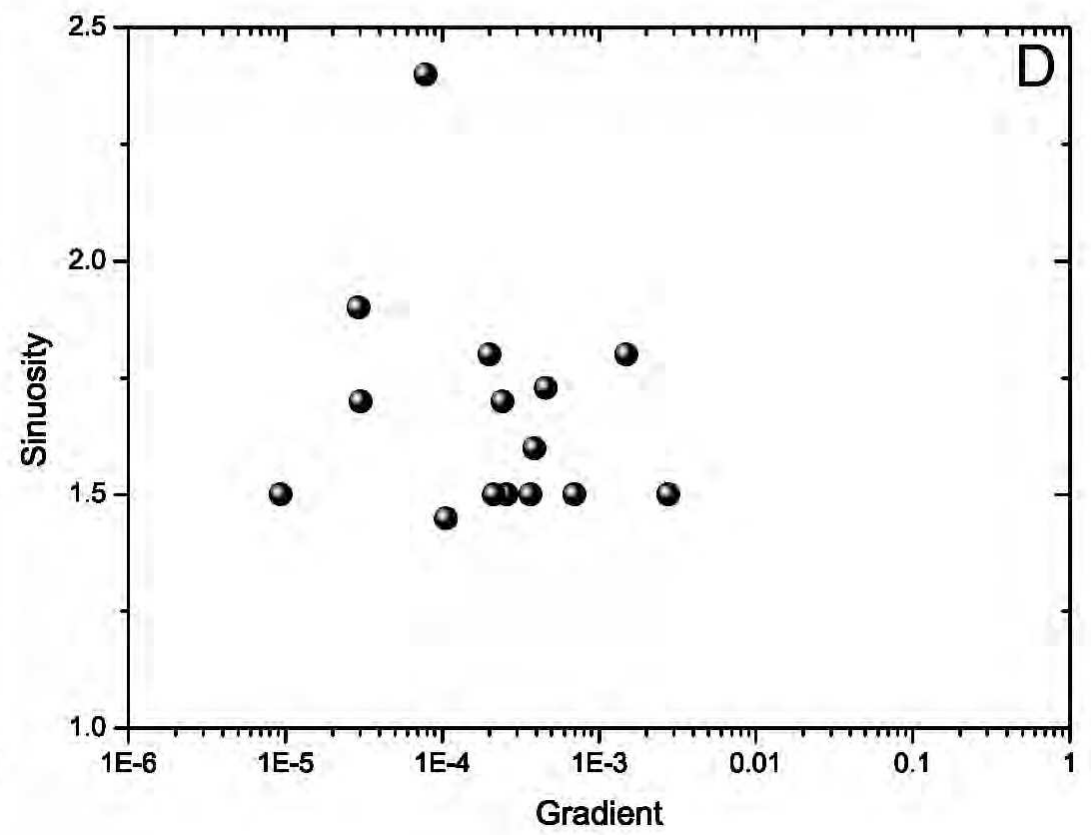
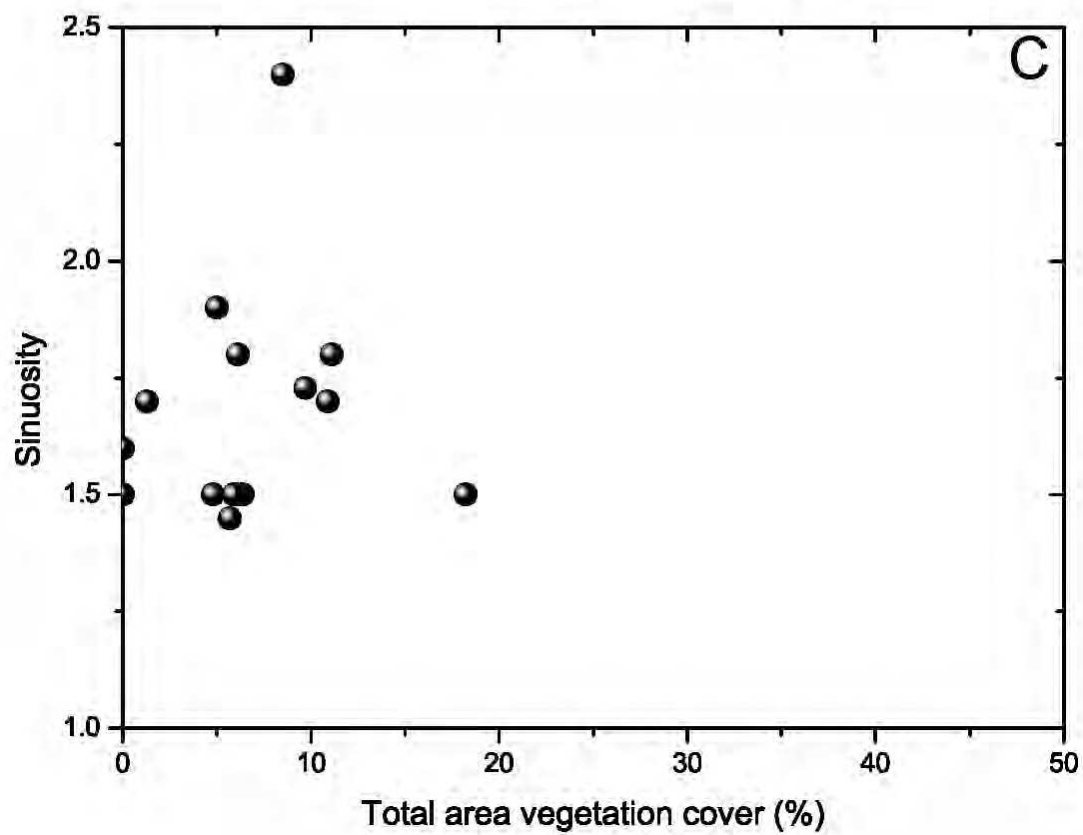
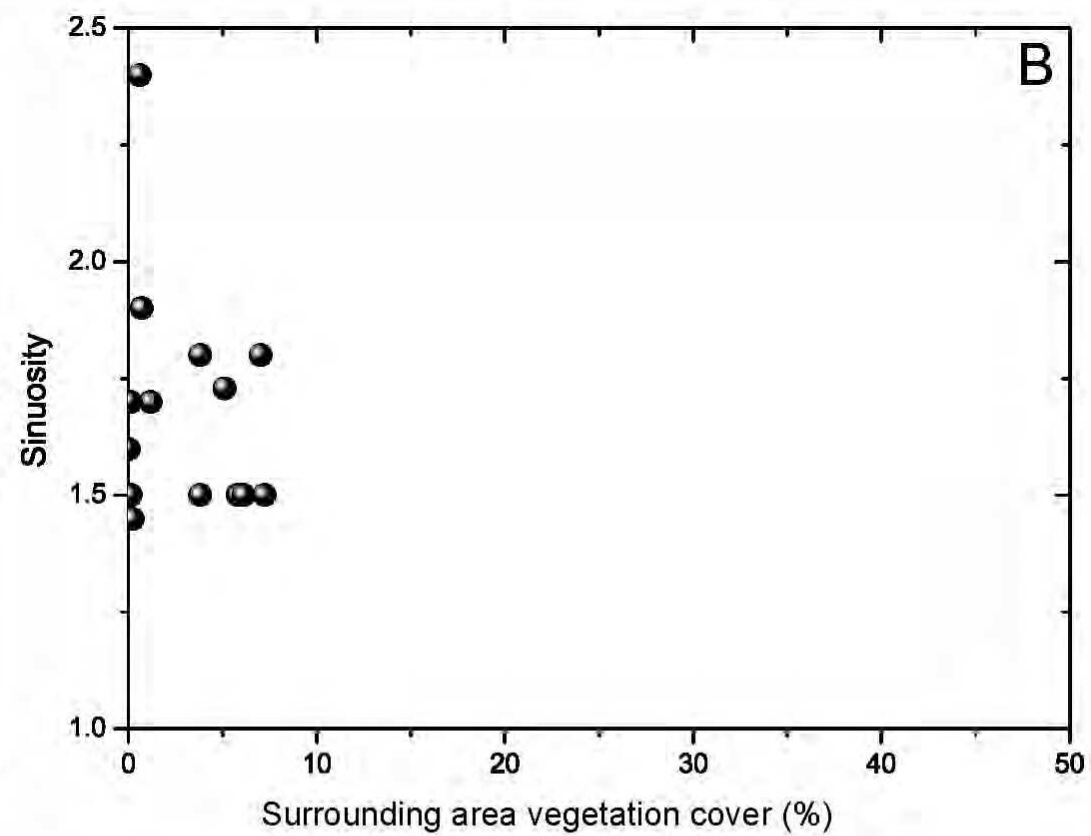
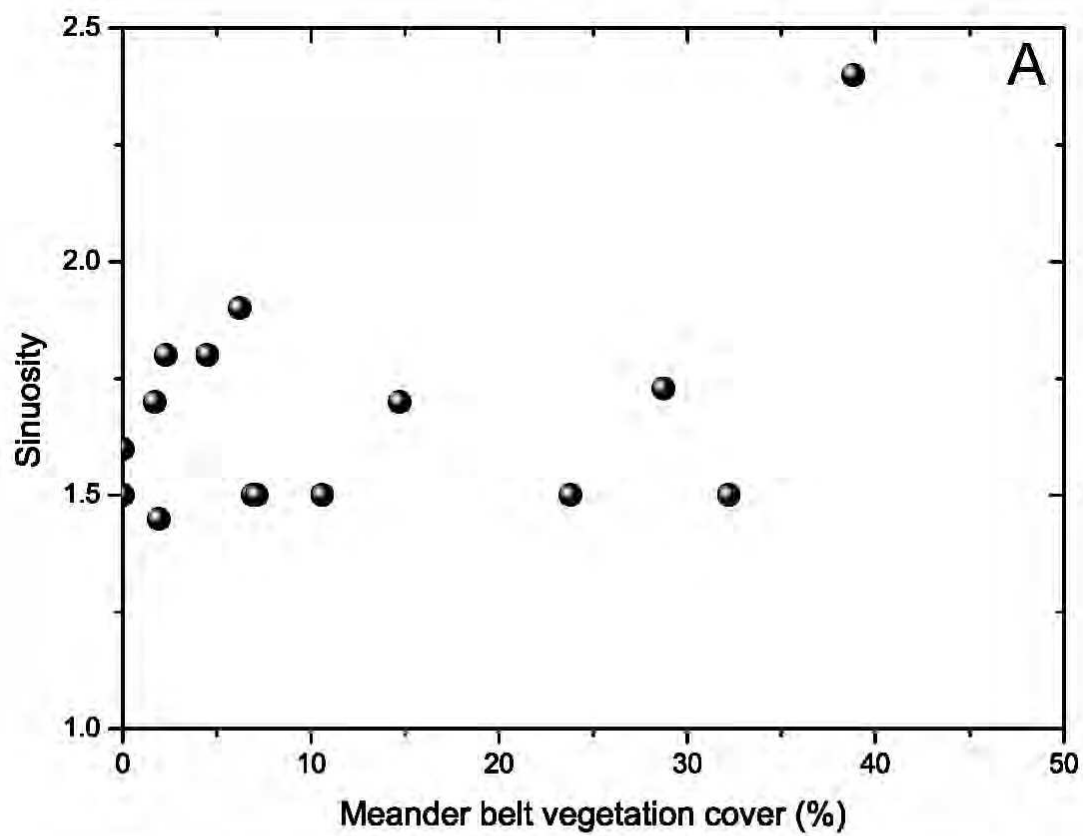


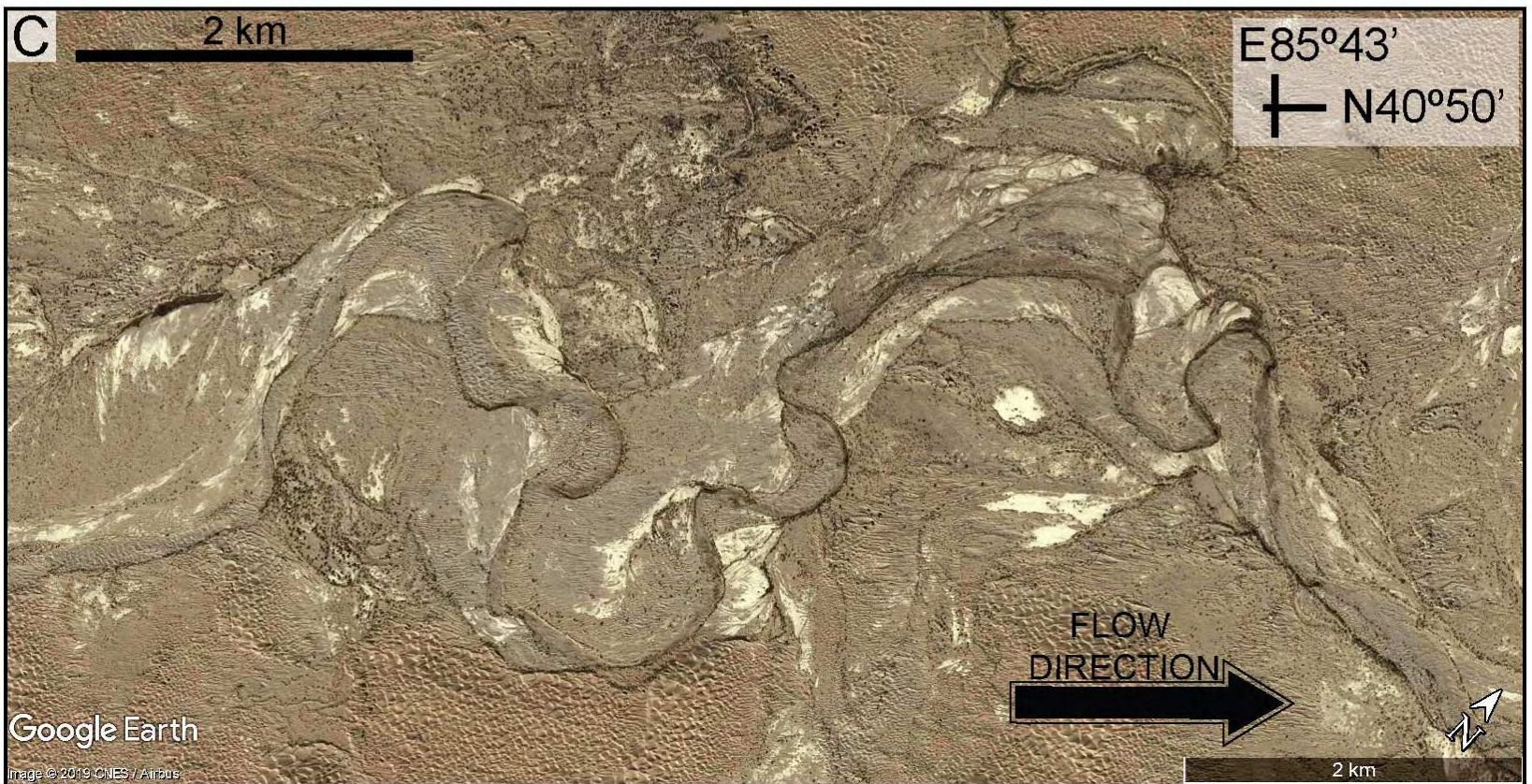
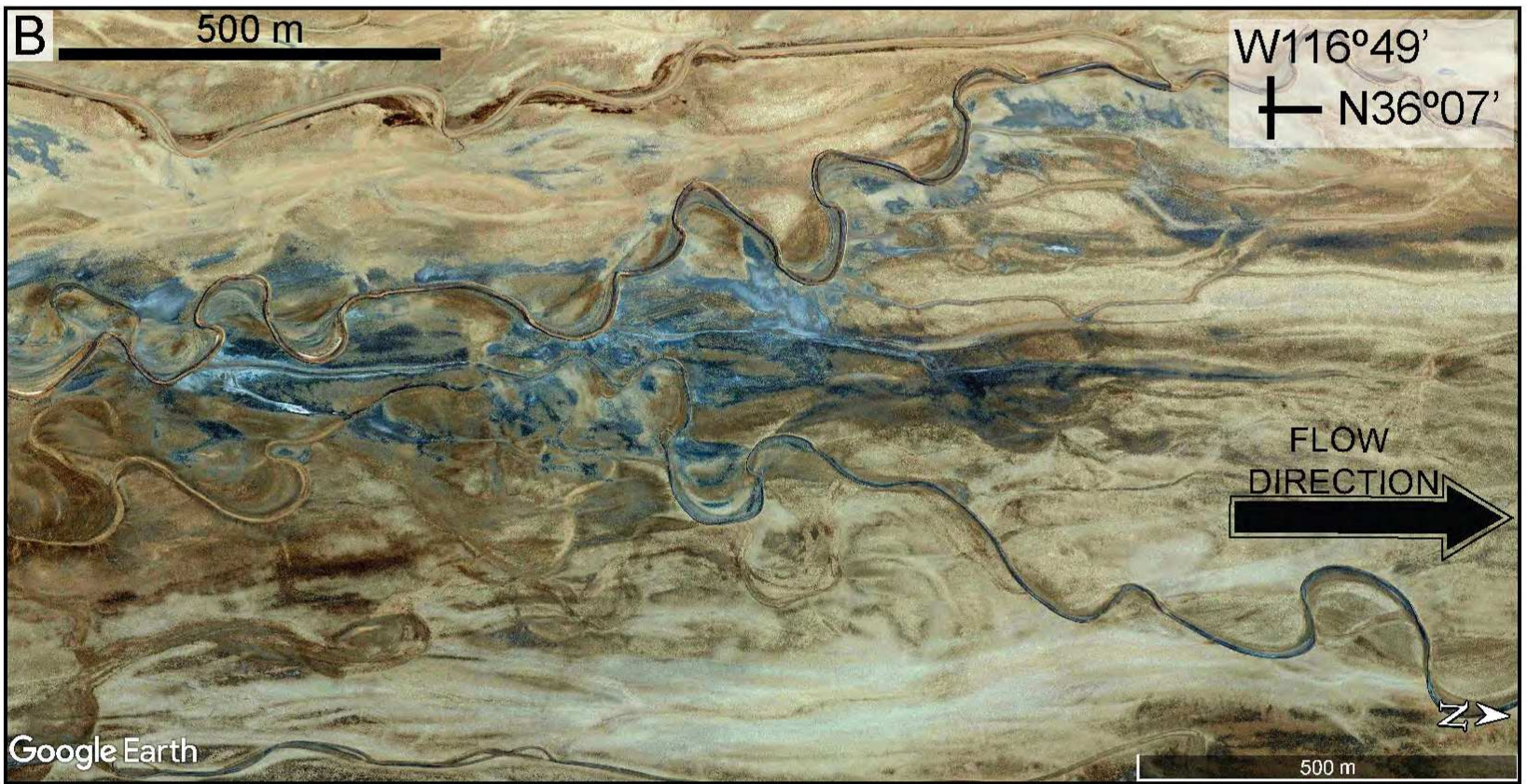
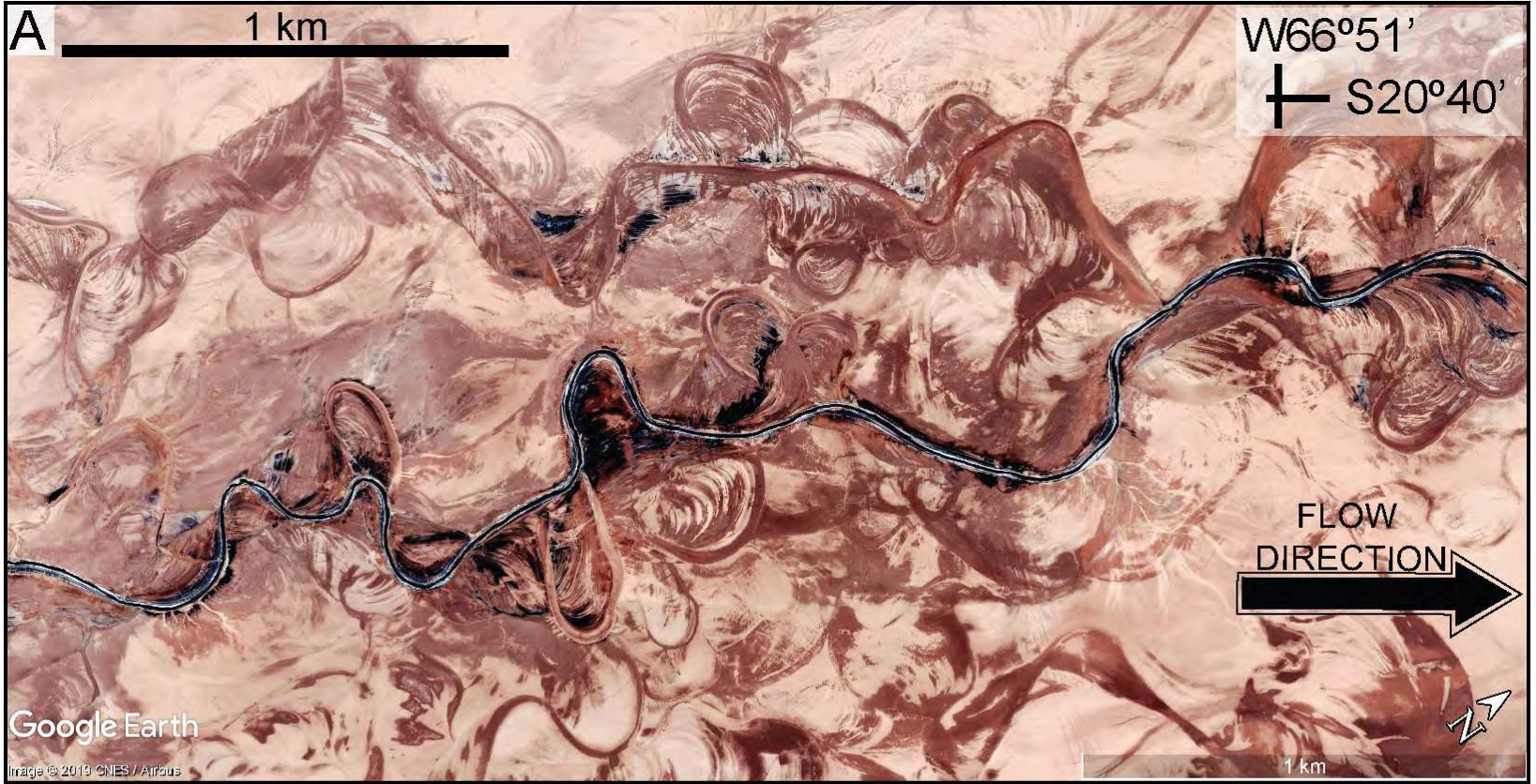


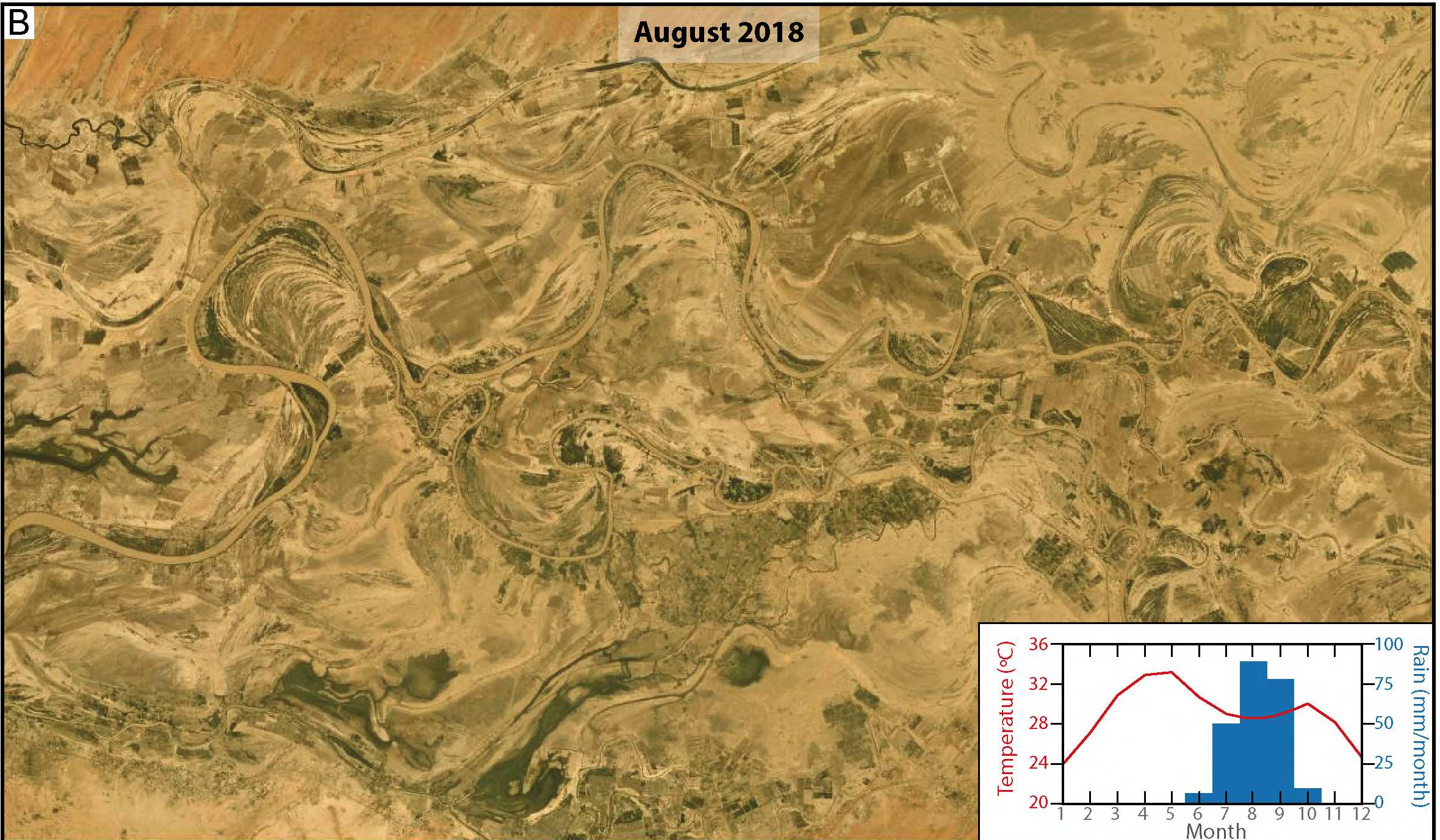












<i>River name</i>	<i>Meander belt length (km)</i>	<i>Thalweg length (km)</i>	<i>Meander belt width average (km)</i>	<i>Meander width average (m)</i>	<i>Sinuosity</i>	<i>Gradient</i>	<i>Total area vegetation cover (%)</i>	<i>Meander belt vegetation cover (%)</i>	<i>Lateral area vegetation cover (%)</i>	<i>Aeolian dunes</i>	<i>Climate</i>	<i>Basin settings</i>	<i>Satellite image</i>
Algeria	44	77	1	37	1.8	0.001493	11.1	4.5	7.0	-	BWh	endorheic intracratonic	LS8 OLI
Altiplano	19	28	0.7	15	1.5	0.000256	0.0	0.0	0.0	-	BWk	endorheic foreland	GeoCover
Amargosa	10	16	-	10	1.6	0.000384	0.0	0.0	0.0	-	BWh	endorheic pull-apart	GeoCover
Batha	230	340	5	126	1.5	0.000362	6.4	7.1	6.1	-	BWh	endorheic intracratonic	GeoCover
Bermejo	75	114	1	60	1.5	0.002773	6.0	6.9	5.8	-	BWk	endorheic intracratonic	GeoCover
Chad 1	141	274	15	220	1.9	0.000029	5.0	6.2	0.7	x	BWh	endorheic intracratonic	GeoCover
Helmand	333	485	4	105	1.5	0.000694	4.8	23.8	0.1	x	BWh	endorheic intracratonic	LS8 OLI
Indus	191	277	60	929	1.5	0.000009	18.2	32.2	7.2	x	BWh	exorheic intracratonic	LS8 OLI
Niger	-	-	4	-	-	0.000221	0.0	0.0	0.0	x	BWh	endorheic intracratonic	GeoCover
Senegal	366	625	17	267	1.7	0.000030	10.9	14.7	0.1	x	BWh	exorheic intracratonic	LS8 OLI
Taklamakan 1	69	111	4	218	1.7	0.000243	1.3	1.7	1.2	x	BWk	endorheic foreland	LS8 OLI
Taklamakan 2	42	61	3	52	1.5	0.000213	5.9	10.6	3.8	x	BWk	endorheic foreland	GeoCover
Turkmenistan 2	81	140	4	123	1.7	0.000457	9.7	28.7	5.1	-	BWk	endorheic intracratonic	GeoCover
Warburton	142	206	2	30	1.5	0.000106	5.7	1.9	0.2	x	BWh	endorheic intracratonic	GeoCover
Yobe	295	630	6	31	2.4	0.000078	8.5	38.8	0.6	x	BWh	endorheic intracratonic	LS8 OLI
Zhanadarya	204	375	19	157	1.8	0.000199	6.1	2.3	3.8	x	BWk	endorheic intracratonic	GeoCover

# Supplementary

## Meandering rivers in modern desert basins: implications for the prevegetation fluvial rock record

Maurício G.M. Santos, Adrian J. Hartley, Nigel P. Mountney, Jeff Peakall, Amanda Owen, Eder R. Merino, and Mario L. Assine

Corresponding author: Mauricio G.M. Santos  
Email: santos.mauricio@ufabc.edu.br

### This PDF file includes:

1. Methodology
2. Meandering rivers in desert basins
3. Studied rivers locations
4. Multi-temporal imagery links

### 1. Methodology

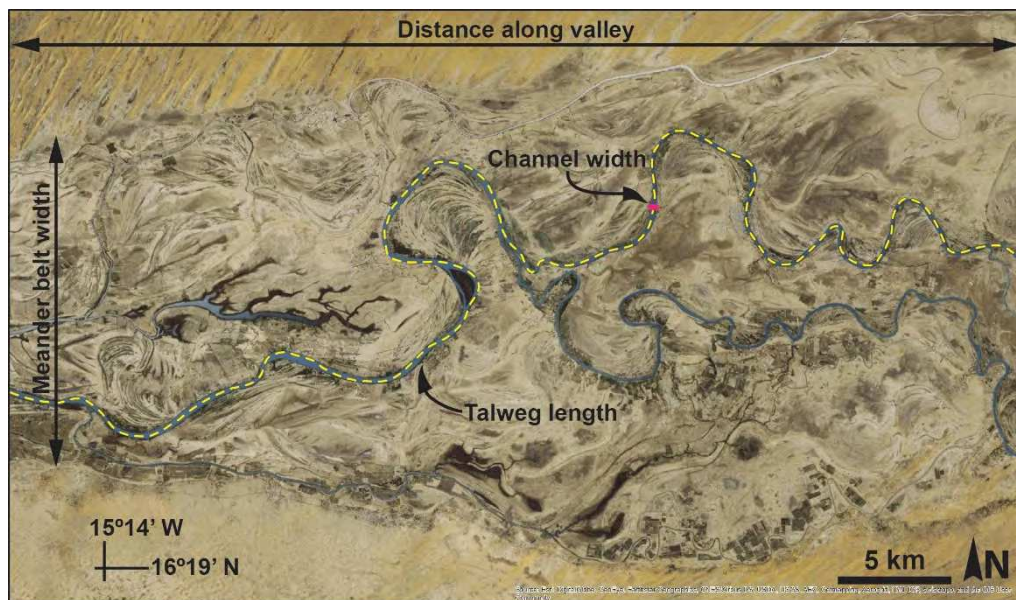


Fig. S1: Methodology of extracted morphometric data, Senegal River.

### 2. Meandering Rivers in Desert Basins

The following images show the areas selected for meander-belt vegetation cover classification (where applicable), with meander-belts contour highlighted. Vegetation-cover values refer to presence of vegetation on meander-belts. See Table 1 for further details.

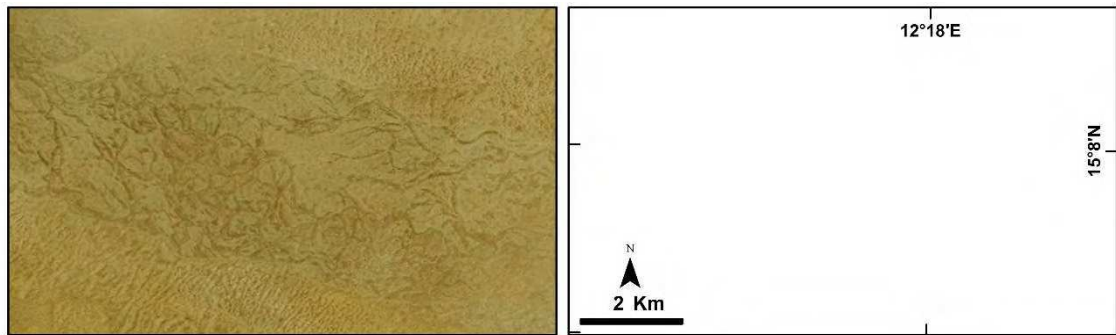


Fig. S2: Sahara Desert (Niger), no vegetation cover.

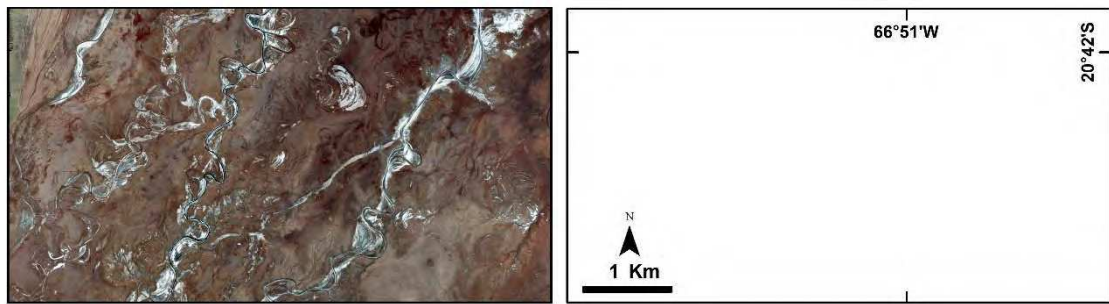


Fig. S3: Altiplano (Bolivia), no vegetation cover.

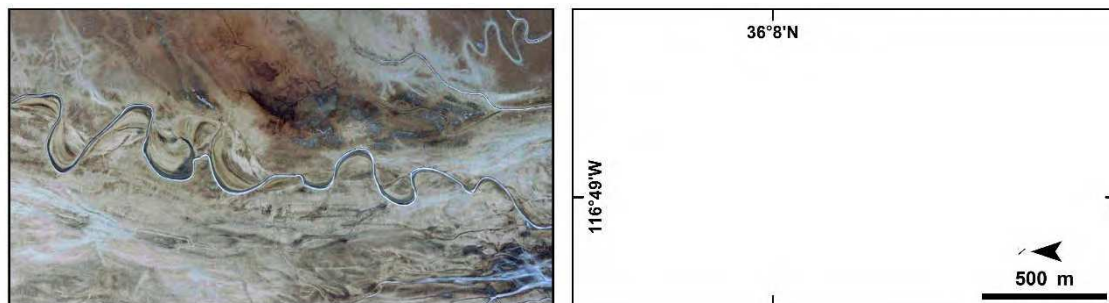


Fig. S4: Amargosa River, Death Valley (USA), no vegetation cover.

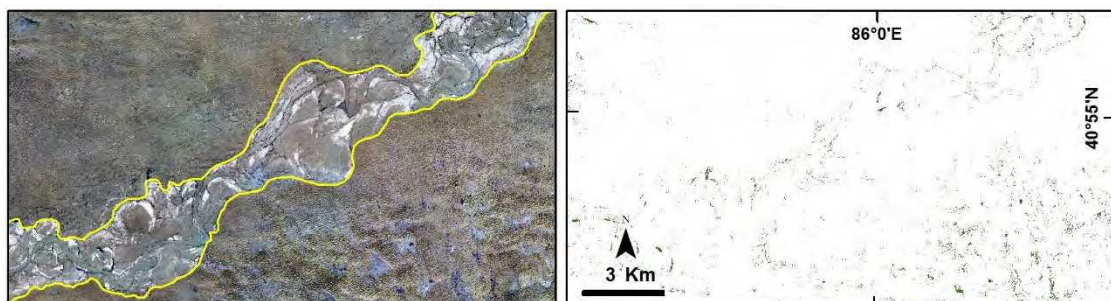


Fig. S5: Taklamakan Desert (China), 1.7% vegetation cover.

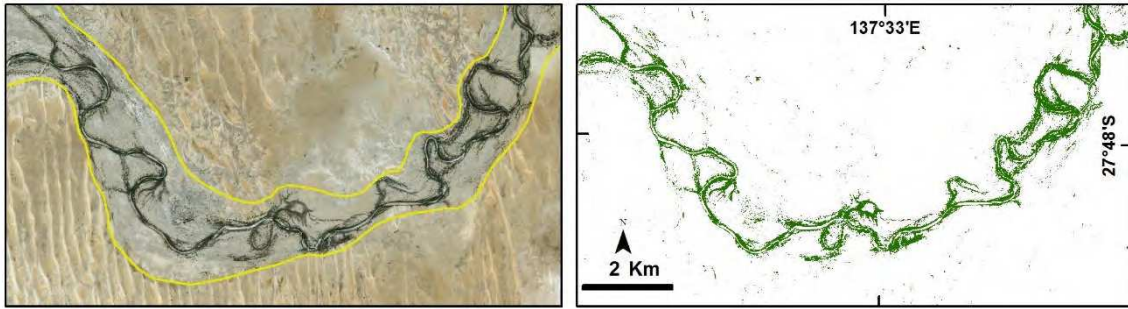


Fig. S6: Warburton River, Lake Eyre (Australia), 1.9% vegetation cover.

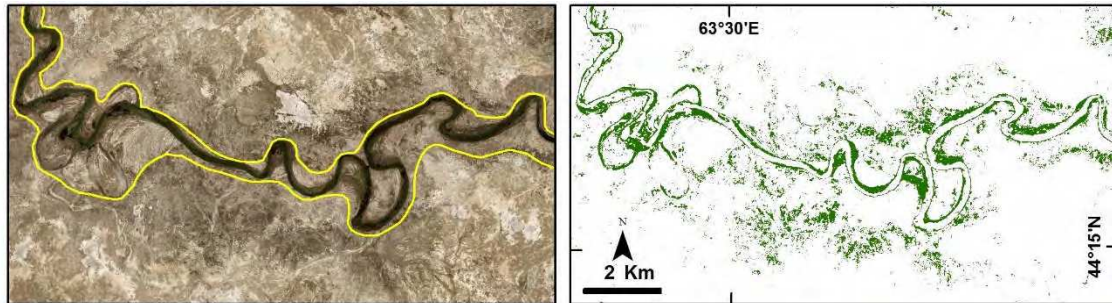


Fig. S7: Zhanadarya River (Kyzylorda, Kazakhstan), 2.3% vegetation cover.

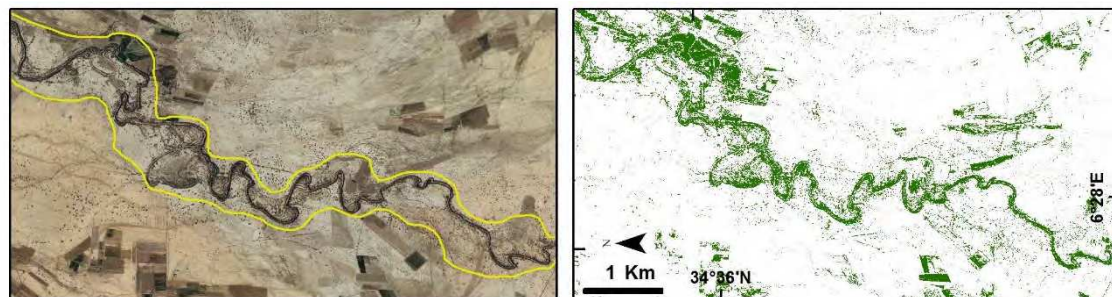


Fig. S8: Sahara Desert, Algeria, 4.5% vegetation cover.

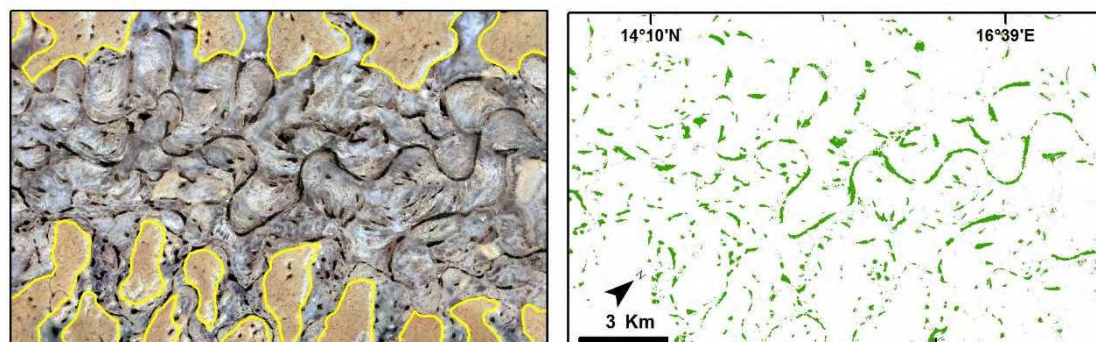


Fig. S9: Sahara Desert (Chad 1), 6.2% vegetation cover.

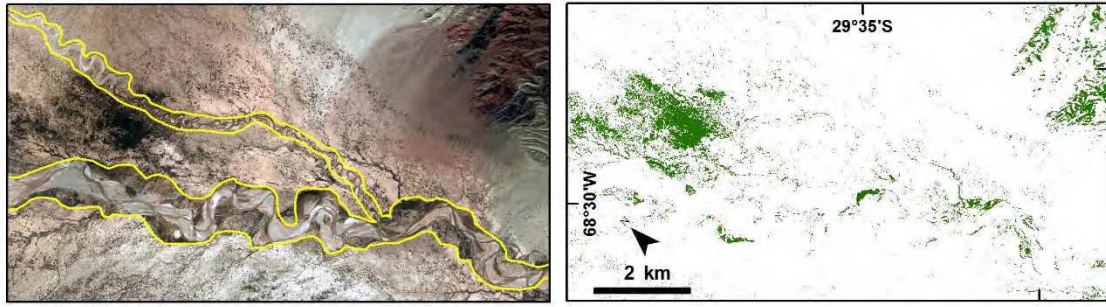


Fig. S10: Bermejo River (Argentina), 6.9% vegetation cover.

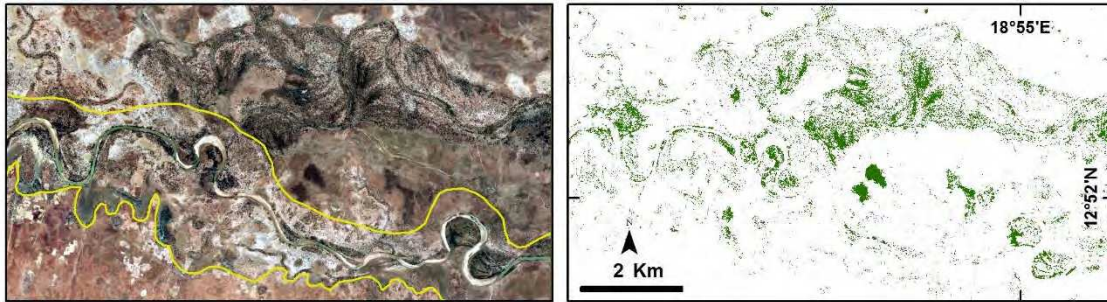


Fig. S11: Sahara Desert, Batha River (Chad 2), 7.1% vegetation cover.

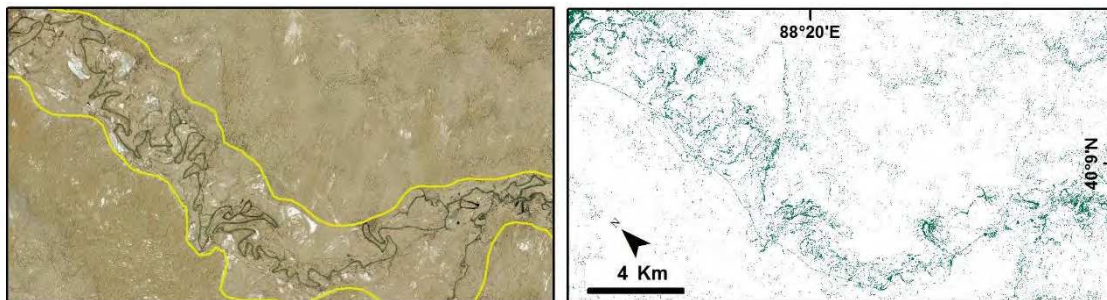


Fig. S12: Taklamakan 2 (China), 10.6% vegetation cover.

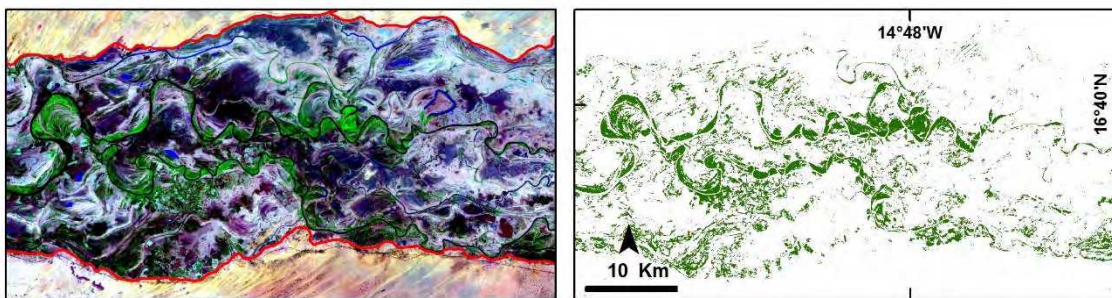


Fig. S13: Sahara Desert, Senegal River (Senegal/Mauritania), 14.7% vegetation cover.

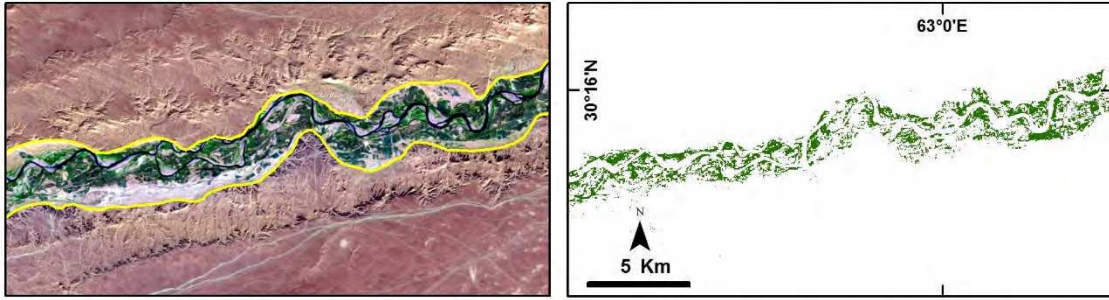


Fig. S14: Helmand River, Margo Desert (Afghanistan), 23.8% vegetation cover.

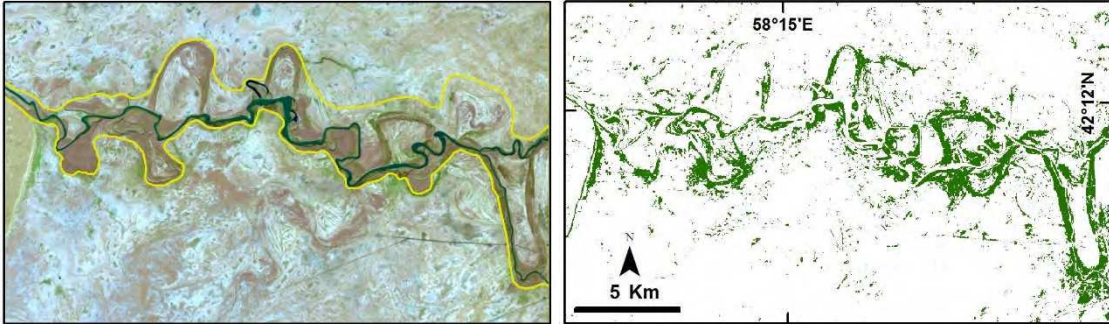


Fig. S15: Sarygamysh Lake Basin (Turkmenistan 2), 28.7% vegetation cover.

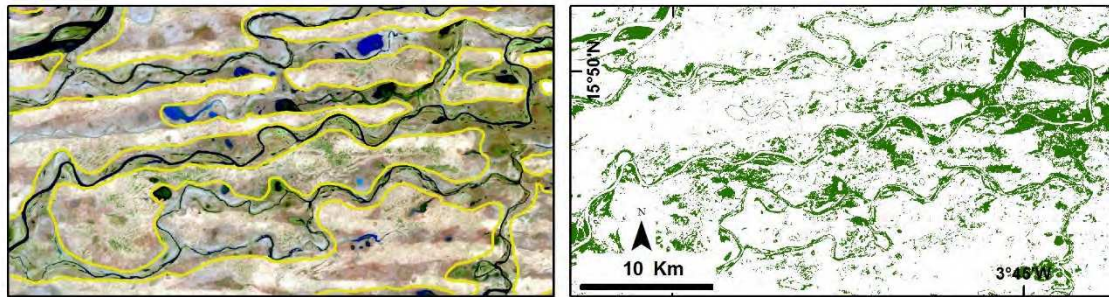


Fig. S16: Sahara Desert, Inner Niger Delta (Mali), 32.2% vegetation cover.

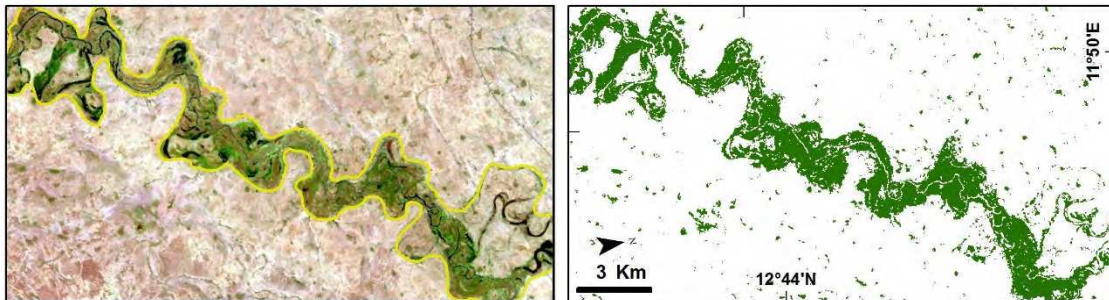


Fig. S18: Sahara Desert, Yobe River (Nigeria), 38.8% vegetation cover.

### 3. STUDIED RIVERS LOCATIONS

	<u>Latitude</u>	<u>Longitude</u>
<b>01. Niger</b>	15°06'52"N	012°20'50"E
<b>02. Altiplano</b>	20°41'23"S	066°50'32"W
<b>03. Death Valley</b>	36° 08'16"N	116°48'34"W
<b>04. Tarim Desert</b>	40°51'41"N	085°51'05"E
<b>05. Helmand River</b>	30°35'50"N	064°00'47"E
<b>06. Chad 1</b>	13°54'55"N	016°22'18"E
<b>07. Warburton River</b>	27°47'02"S	137°29'40"E
<b>08. Tarim Desert 2</b>	40°29'16"N	087°57'51"E
<b>09. Bermejo River</b>	29°36'24"S	068°28'12"W
<b>10. Kyzylorda</b>	44°19'02"N	063°12'47"E
<b>11. Chad 2</b>	13°12'02"N	018°22'16"E
<b>12. Turkmenistan 2</b>	42°11'52"N	057°58'30"E
<b>13. Senegal River</b>	16°39'10"N	014°55'19"W
<b>14. Yobe River</b>	13°07'16"N	012°16'55"E
<b>15. Algeria</b>	34°36'55"N	006°32'01"E
<b>16. Inner Niger Delta</b>	15°47'55"N	003°51'47"W

#### 4. MULTI-TEMPORAL IMAGERY LINKS

01. Niger

<https://earthengine.google.com/timelapse/#v=14.90853,12.50427,11.061,latLng&t=0.51>

02. Altiplano (Bolivia)

<https://earthengine.google.com/timelapse/#v=-20.67891,-66.83777,11.973,latLng&t=0.37>

03. Death Valley (USA)

<https://earthengine.google.com/timelapse/#v=36.12278,-116.78864,11.973,latLng&t=1.60>

04. Tarim 1 (China)

<https://earthengine.google.com/timelapse/#v=40.93444,86.05131,11.973,latLng&t=0.18>

05. Helmand River (Afghanistan)

<https://earthengine.google.com/timelapse/#v=30.49586,63.58401,10.363,latLng&t=1.88>

06. Chad 1

<https://earthengine.google.com/timelapse/#v=14.32081,16.85321,9.249,latLng&t=3.24>

07. Warburton River (Australia)

<https://earthengine.google.com/timelapse/#v=-27.74545,137.74205,11.106,latLng&t=3.13>

08. Tarim 2 (China)

<https://earthengine.google.com/timelapse/#v=40.47666,87.91626,10.17,latLng&t=1.65>

09. Bermejo River (Argentina)

<https://earthengine.google.com/timelapse/#v=-29.70231,-68.41044,11.973,latLng&t=2.06>

10. Kyzylorda (Kazakhstan)

<https://earthengine.google.com/timelapse/#v=44.35814,63.75796,9.87,latLng&t=3.20>

11. Chad 2

<https://earthengine.google.com/timelapse/#v=13.26351,19.7962,9.362,latLng&t=3.24>

12. Turkmenistan 2

<https://earthengine.google.com/timelapse/#v=42.18849,58.12493,10.404,latLng&t=1.83>

13. Senegal River (Senegal/Mauritania)

<https://earthengine.google.com/timelapse/#v=16.63686,-15.00031,9.874,latLng&t=2.79>

14. Yobe River (Nigeria)

<https://earthengine.google.com/timelapse/#v=13.02792,12.14021,9.51,latLng&t=1.18>

15. Algeria

<https://earthengine.google.com/timelapse/#v=34.59697,6.49548,11.848,latLng&t=1.02>

16. Inner Niger Delta (Mali)

<https://earthengine.google.com/timelapse/#v=15.68361,-3.97495,8.982,latLng&t=0.00>

## APPLICATION REFERENCES

- Arababah, M.A., and M.N. Alhamad. 2006. Land use/cover classification of arid and semi-arid Mediterranean landscapes using Landsat ETM. *International Journal of Remote Sensing* 27: 2703–2718 - *used unsupervised and supervised classification methods to map land use, and showed that supervised classification improved map accuracy*
- Eve, M.D., W.G. Whitford, and K.M. Havstad. 1999. Applying satellite imagery to triage assessment of ecosystem health. *Environmental Monitoring and Assessment* 54: 205–227 – *used supervised classification to map irreversibly degraded rangelands*
- Hudak, A.T., and B.H. Brockett. 2004. Mapping fire scars in a southern African savannah using Landsat imagery. *International Journal of Remote Sensing* 25: 3231–3243 – *used supervised classification to map fire burn severity*
- Lauver, C.L. 1997. Mapping species diversity patterns in the Kansas shortgrass region by integrating remote sensing and vegetation analysis. *Journal of Vegetation Science* 8: 387–394 – *used supervised classification to differentiate high and low quality grasslands*
- Yüksel, A., A.E. Akay, and R. Gundogan. 2008. Using ASTER Imagery in Land Use/cover Classification of Eastern Mediterranean Landscapes According to CORINE Land Cover Project. *Sensors* 8: 1237–1251 – *used supervised classification to map major land use types*

## TECHNICAL REFERENCES

- Cingolani, A.M., D. Renison, M.R. Zak, and M.R. Cabido. 2004. Mapping vegetation in a heterogeneous mountain rangeland using landsat data: an alternative method to define and classify land-cover units. *Remote Sensing of Environment* 92: 84–97.
- Congalton, R.G. 1991. A review of assessing the accuracy of classifications of remotely sensed data. *Remote Sensing of Environment* 37:35–46.
- Geerken, R., B. Zaitchik, and J.P. Evans. 2005. Classifying rangeland vegetation type and coverage from NDVI time series using Fourier Filtered Cycle Similarity. *International Journal of Remote Sensing* 26: 5535–5554.
- Ghorbani, A., D. Bruce, and F. Tiver. 2006. Specification: A problem in rangeland monitoring. In: *Proceedings of the 1st International Conference on Object-based Image Analysis (OBIA)*, 4th–5th July 2006, Salzburg, Austria.
- Jensen, J. R. (2009). *Remote sensing of the environment: An earth resource perspective 2/e*, Prentice Hall.
- Karl, J. W., and B. A. Maurer. 2009. Multivariate correlations between imagery and field measurements across scales: comparing pixel aggregation and image segmentation. *Landscape Ecology*. DOI: 10.1007/s10980-009-9439-4.

Leopold, L. B., Wolman, M. G., and Miller, J. P. (1964). "Fluvial processes in geomorphology," W. H. Freeman and Company, San Francisco, California.